MONTHLY NOTICES

OF THE

ROYAL ASTRONOMICAL SOCIETY

Vol. 108 • No. 2

MEETING OF 1948 MARCH 12

Professor W. M. H. Greaves, President, in the Chair

The election by the Council of the following Fellows was duly confirmed, the names of the proposers from personal knowledge being appended :—

Alan Stewart Curry, B.A., 86 Watson Road, Blackpool (proposed by P. J. Melotte);

Nicholas John Kolatschevsky, L.Sc.C., 119 Brecknock Road, London, N. 19 (proposed by A. D. Thackeray);

Harold M. Stanier, 6 St. John's Road, Cambridge (proposed by A. D. Thackeray); and

Gerd Bernard Wellgate, Cornerways, Abinger, Surrey (proposed by R. d'E. Atkinson).

The election by the Council of the following Junior Members was duly confirmed, the names of the proposers from personal knowledge being appended:—

Peter Lancaster Brown, 3 Sunnyside Terrace, Colindale, London, N.W. 9 (proposed by K. F. Stonebridge);

Sidney Nevil Milford, 33 Arkwright Road, London, N.W. 3 (proposed by H. S. W. Massey); and

Alan John Oldham, B.A., Albert House, Hyde, Cheshire (proposed by D. W. Dewhirst).

Ninety presents were announced as having been received since the last meeting, including:—

M. G. J. Minnaert, G. F. W. Mulders and G. Houtgast, *Photometric Atlas of the Solar Spectrum*, presented by M. G. J. Minnaert;

J. B. Sidgwick, *The Heavens Above*, presented by the author;

Jahrbuch der Preussischen Kunstsammlungen, presented by Mr D. H. Sadler; and

Observations Ionospheriques et Solaires, presented by Dr R. d'E. Atkinson.

THE APPLICATION OF THE NATIONAL ACCOUNTING MACHINE TO THE CALCULATION OF APPARENT PLACES OF STARS

H. W. P. Richards and D. H. Sadler

(Communicated by the Astronomer Royal)

(Received 1948 February 4)

Summary

A method is developed for the systematic calculation of apparent places of stars, using the National Accounting Machine. Checked copy, printed by the machine in precisely the form required by the printer, is produced in a time which compares favourably with other methods.

---

1. *Introduction.*—It is required to produce values of the apparent right ascension and declination of a number of stars at the (different) times of their upper transits over the meridian of Greenwich on every tenth day throughout the year. This involves the formation of a series of products of constants and varying factors, and would appear to imply the necessity of many multiplications (about 300 for each star). The National machine, as described below (Section 2), seems completely unsuitable for this work, but circumstances arose that made it necessary to devise a method that could be used on that machine. This has proved so successful—the method produces "copy" exactly in the form in which it is printed—that it has taken its place as the standard method in the Nautical Almanac Office. The opportunity is now taken to publish it, especially as it would seem to have applications over a much wider field.

2. *The National machine.*—A full description of this machine has been given by Comrie (1), and it is not necessary here to give more than a very brief outline of its functions and capabilities. The National is a printing adding machine with six adding mechanisms ("registers"), two of which, Nos. 1 and 3, will subtract directly, as well as add. (The other four registers will subtract by addition of complements.) A number set on the 12-figure keyboard can be added (including subtraction in registers 1 and 3) to any combination of the six registers; the contents of any register can be transferred, either with clearing (a "Total" or T operation) or without clearing (a "Sub-Total" or ST operation) of the register selected, to any combination of registers. Printing takes place at each operation unless deliberately suppressed, either by a special non-print (NP) arm attached to the stops, or casually by hand; printing can also be partially suppressed by the use of a ½NP arm, and (in all positions) by a non-print slide.

The destination of a number is controlled by the "stop" on which the machine is operated, and thus by the position of the moving carriage; stops can be made available for any combination of registers. The source of a number, if not the keyboard, is a register selected by the operator, but a standard cycle of operations is used as far as possible, so that register selection is normally also largely governed by carriage position.

The moving carriage bears a removable "form-bar" on which stops can quickly be placed in any desired position and order; it normally "tabulates", or moves from one stop to the next, after each operation, while a return (R) stop at the

end of a line causes the carriage to return to the beginning of the line, indicated by a margin (M) stop, with automatic paper-feeding.

The following special features of the machine, which are directly used in the present method, should be mentioned here. A "non-add" (0) stop permits printing of figures without transfer to any register; the two subtracting registers (1 and 3) can be controlled by "reversible" stops, so that an immediate change may be made from addition to subtraction, or *vice versa*. The machine can be made to interpret an instruction to subtract the contents of a register from itself as an instruction to clear that register.

3. *Outline of method.*—The principle of the method to be described is the fact that multiplication of a constant by a series of numbers can be replaced by continued addition of the products of the constant by the first differences of the series. This principle can clearly be extended to second, third and higher differences, and also to more than one such series of products.

Moreover, interpolation to a fixed interval can be performed by addition of the products of (fixed) interpolation coefficients and a series of high-order differences of the function.

4. *Notation and formulae.*—In the usual notation (see, for instance, the *Nautical Almanac* for 1948, page 592) the apparent place of a star at any time is given by

$$\alpha = \alpha_0 + \tau\mu_\alpha + E + Aa + Bb + Cc + Dd + \text{parallax} + \text{orbital motion} \qquad (1)$$

$$\delta = \delta_0 + \tau\mu_\delta + Aa' + Bb' + Cc' + Dd' + \text{parallax} + \text{orbital motion} \qquad (2)$$

Here the "star constants" a, b, c, d, a', b', c', d', although strictly dependent on α and δ, can, for stars not too close to the poles, be treated as constants throughout the year. The Besselian Day Numbers A, B, C, D are independent of the particular star; but as the apparent place is to be calculated for the time of transit at Greenwich, which depends upon the right ascension, the values required are different for every star. E, which occurs in the right ascension only, is a small slowly varying quantity, τ is the fraction of the year and μ is the annual proper motion.

The corrections for parallax may be put into the form

$$\Delta\alpha = \pi(cY - dX) \qquad \Delta\delta = \pi(c'Y - d'X) \qquad (3)$$

where π is the annual parallax and X, Y are two of the Sun's equatorial rectangular coordinates. To a sufficient approximation X, Y are proportional to C, D, being dependent on the cosine and sine of the Sun's longitude. The corrections may therefore be combined with the terms $Cc + Dd$, $Cc' + Dd'$ in (1) and (2) by replacing the star constants c, d, c', d' by the expressions $c + d\pi k_1$, $d - c\pi k_2$, $c' + d'\pi k_1$, $d' - c'\pi k_2$ respectively, in which

$$k_1 = \frac{R}{k\cos\epsilon} \qquad k_2 = \frac{R\cos\epsilon}{k}$$

where R is the Sun's radius vector, ϵ the obliquity, and k the constant of aberration, $20''{\cdot}47$. The maximum variation of R from its mean value of unity is $\pm 1/60$, and no appreciable error is introduced (except in very extreme cases) by neglecting this variation.

The corrections for orbital motion, which are only applicable to a very small number of stars, can be treated as linear without sensible error over a period of a year.

The above formula for right ascension is now put into the following form, in order to facilitate the application of the principles of Section 3 (the similar transformation for declination will be evident, but it must be pointed out that in the case of negative declinations the signs of the star constants a', b', c', d' are reversed and the seconds of declination are treated as positive):

$$\alpha = F + G \tag{4}$$

where

$F = f$, interpolated systematically to the time of transit

$$f = p \times 2A + 2b \times \tfrac{1}{2}B + 2(c + d\pi k_1) \times \tfrac{1}{2}C + 2(d - c\pi k_2) \times \tfrac{1}{2}D \tag{5}$$

(calculated for 12^h Greenwich Sidereal Time)

p = rounded-off value of $\frac{1}{2}(a + e\psi)$

where

$e\psi = E/(A - \tau)$ may be taken as a constant $= 0{\cdot}00768$

$$G = \alpha_0 + \tau(\mu_\alpha - e\psi) + 2A\{\tfrac{1}{2}(a + e\psi) - p\} + 0^s{\cdot}0005 + \text{orbital motion} \tag{6}$$

in which α_0 is the mean place at the beginning of the (Besselian fictitious) year, the next two terms include the effects of proper motion and (with $p \times 2A$ from f) of precession, and the constant $0^s{\cdot}0005$ is introduced, as is usual in mechanical integration, in order to round off all values automatically to the nearest (published) unit. All these terms can be treated as linear with negligible error, and the values of G are therefore calculated for the initial and final dates only, and a constant first difference is determined from these limiting values. It should also be noted that the values of G are not affected by the interpolation to time of transit by which F is determined from f, and they must therefore be calculated (with values of τ and $2A$) for the actual time of transit of the star.

It will be noticed that the four main products have been rearranged to minimize the effect of the rounding-off of the separate factors, by equalizing (approximately) their maxima; since the principal part of A is linear, the effect of the rounding-off of p can be allowed for in G, although no great error would be caused by its neglect. The number of decimals in each product must, of course, be the same. The splitting of E into the difference between two large quantities is a computational simplification; there is no corresponding term in e in the declination.

It was pointed out in Section 1 that the right ascension and declination are required at every tenth upper transit over the Greenwich meridian, and the series commences with the transit that takes place within the twenty-four hours between 0^h Greenwich Sidereal Time on January 0 and 0^h G.S.T. on January 1. This date is known (for the present purpose) as day 0, and the arguments used in the National "set-up" (Section 8) are therefore multiples of 10 from 0 to 370, with one additional value at each end to permit of the evaluation of the first differences preceding the first, and succeeding the last, printed value of the function. The initial and final values of G are thus calculated for dates -10 and 380, and the (constant) first difference is found from

$$g = \frac{1}{39}(G_{380} - G_{-10}) \tag{7}$$

The value of g used in the computation is that determined from (7) suitably rounded off; a value of G_{check}, calculated as

$$G_{\text{check}} = G_{-10} + 39g$$

where g takes the rounded-off value, is found for inclusion in the final value of the function to be reproduced by the National machine.

The usual central-difference notation is used, with obvious modifications to the suffixes on account of the 10-day interval:

Argument	Function		Differences		
-10	f_{-10}		δ^2_{-10}		δ^4_{-10}
		δ'_{-5}		δ^3_{-5}	
0	f_0		δ^2_0		δ^4_0
		δ'_{+5}		δ^3_{+5}	
$+10$	f_{+10}		δ^2_{+10}		δ^4_{+10}

In order to combine the advantages of a single fixed set of Day Numbers with the theoretical necessity of a different set for each star, the function f defined in (5) is calculated at intervals of 10 sidereal days from 12^h Greenwich Sidereal Time on day 0, and then interpolated, with interpolating factor $2r$ given by

$$2r = \frac{1}{240}(\alpha_0 - 12^h) \tag{8}$$

to give F, which thus corresponds to the time of transit of the star. The maximum value of $2r$ is clearly $\pm 0{\cdot}05$.

The calculation of f is made by integration from its fourth differences

$$\delta^4 f = p \times \delta^4(2A) + 2b \times \delta^4(\tfrac{1}{2}B) + 2(c + d\pi k_1) \times \delta^4(\tfrac{1}{2}C) + 2(d - c\pi k_2) \times \delta^4(\tfrac{1}{2}D) \tag{9}$$

in which the fourth differences of the Day Numbers are those of a set independent of the star, calculated for 12^h Greenwich Sidereal Time on the dates required.

The interpolation of f with the constant interpolating factor $2r$ to give F is performed by means of Stirling's formula

$$F_0 = f_0 + r(\delta'_{-5} + \delta'_{+5}) + 2r^2\delta^2_0 + \ldots \tag{10}$$

in which the second-order term is negligible owing to the small range of r.

If the first difference of α be denoted by Δ, then we have, for typical arguments,

$$\Delta_5 = \delta'_5 + r(\delta^2_0 + \delta^2_{10}) + g \tag{11}$$

For reasons that will become apparent later, successive values of Δ and α are actually formed on the National machine (Section 8) by means of:

$$\Delta_{15} = \Delta_5 + \delta^2_{10} + r\delta^3_5 + r\delta^3_{15} \tag{12}$$

$$\alpha_{20} = \alpha_{10} + \Delta_{15} \tag{13}$$

The values of δ^2 and δ^3 are, of course, built up from relations of the form:

$$\delta^3_{15} = \delta^3_5 + \delta^4_{10}; \qquad \delta^2_{20} = \delta^2_{10} + \delta^3_{15} \tag{14}$$

5. *Day Numbers.*—A series of values of $2A$, $\frac{1}{2}B$, $\frac{1}{2}C$, $\frac{1}{2}D$, is determined at interval 10 sidereal days throughout the year, commencing at 12^h G.S.T. on January -9 (December 22 of the preceding year). These values are differenced as far as the fourth difference and, if necessary, a small number of adjustments, not exceeding one unit in the end figure, is made to reduce the number of changes of sign in the fourth difference. A table of the adjusted fourth differences (see Table I) is supplied to the operator of the National machine. It will be noticed that the fourth differences opposite days 0, 370 and 380, which are not defined by

the calculated Day Numbers, are taken to be zero. Table I also contains values of the six following quantities, used in the calculation of initial settings and check values, for each of the four Day Numbers:

$$\left.\begin{array}{l} U = \text{function value for day } -10 \\ V = \delta'_{-15} + \delta'_{-5}; \quad W = \delta^2_{-10}; \quad X = \delta^3_{-15} \\ Y = \text{function value for day } 380 \\ Z = \delta'_{375} + \delta'_{385} \end{array}\right\} \qquad (15)$$

The unit for $2A$ is 0·0001, while that for the other three Day Numbers is 0″·001; all the quantities in Table I are given as integers in terms of these units.

TABLE I

Fourth differences, and leading values, of Day Numbers at 12^h *G.S.T.*, 1950

Day	$2A$	$\frac{1}{2}B$	$\frac{1}{2}C$	$\frac{1}{2}D$	Day	$2A$	$\frac{1}{2}B$	$\frac{1}{2}C$	$\frac{1}{2}D$
0	0	0	0	0	200	+5	0	+3	−6
10	0	+4	0	+10	210	4	0	2	7
20	+9	+2	−9	9	220	8	+4	5	8
30	9	0	7	9	230	2	−4	5	1
40	5	−2	7	5	240	9	1	4	7
50	10	2	9	3	250	3	2	8	3
60	1	2	10	+3	260	0	5	7	3
70	+3	4	11	−2	270	+2	2	7	−2
80	−2	7	4	1	280	−3	4	9	+2
90	2	0	11	5	290	4	2	9	0
100	6	4	7	4	300	8	4	6	5
110	5	−2	3	5	310	8	−1	12	4
120	8	+2	5	7	320	3	+4	2	8
130	5	0	5	7	330	12	0	9	11
140	3	1	1	5	340	3	4	3	7
150	6	3	1	10	350	1	3	+2	12
160	1	4	−4	4	360	1	9	−1	13
170	−1	2	+4	7	370	0	0	0	0
180	+4	1	0	10	380	0	0	0	0
190	1	6	1	3					

	U	V	W	X	Y	Z
$2A$	− 1996	+1592	− 8	−16	+22087	+1458
$\frac{1}{2}B$	− 4174	− 14	− 38	+ 6	− 4333	− 129
$\frac{1}{2}C$	− 12	−3317	+ 3	+50	− 3851	−3017
$\frac{1}{2}D$	+10234	+ 6	−332	+16	+ 9334	−1489

6. *Star constants and their multiples.*—The star constants b, c, d, b', c', d' are computed at intervals of ten years, using the mean positions of the stars for 1950·0, 1960·0, etc., a check being made by means of a manuscript table (which it is intended to publish in the forthcoming *Supplement* to the *Nautical Almanac*) of the annual variations of star constants. This table gives, for every hour of right ascension, and for declinations $0°(10°) \pm 60°(5°) \pm 80°$, the annual variations of the six star constants. The values of the annual precessions, a and a', are taken from the mean place pages of the volume of *Apparent Places of Fundamental Stars* for the year concerned, these pages being now available in proof form about three years in advance. The quantities actually required for the computation (see (5))

are p, $2b$, $2(c+d\pi k_1)$ and $2(d-c\pi k_2)$, with the corresponding quantities for the declination, and these multiples of the star constants are obtained for each year by interpolation from the ten-yearly values.

For right ascension generally, p is in units of $0^s{\cdot}0001$, while the other three star constants, which contain a factor to convert seconds of arc to time, are numbers in units of $0{\cdot}00001$; thus each of the products in f is in units of the eighth decimal of a second of time. For declinations the corresponding star constants are given to one decimal less and a figure is also dropped for the right ascension when the declination exceeds $\pm 60°$; in both these cases the working unit is thus the seventh decimal.

The next step is to prepare tables of the first 13 integral multiples of the four constants required for each coordinate of each star. It is unnecessary to describe in any further detail the process of continuous addition on the National machine whereby these tables are produced. Fig. 1 shows the table of multiples of the four star constants for the right ascension for 1950 of Star No. 1073 in the FK3 catalogue (268 G. Ceti), reproduced, slightly reduced in size, from the actual figures printed by the National machine. In the calculation (which is not given here) the effect of a parallax of $0''{\cdot}147$ has been included.

10 73

	p	$2b$	$2c$	$2d$
	+	+	+	+
1	158 88	12 20	105 95	82 57
2	317 76	24 40	211 90	165 14
3	476 64	36 60	317 85	247 71
4	635 52	48 80	423 80	330 28
5	794 40	61 00	529 75	412 85
6	953 28	73 20	635 70	495 42
7	1 112 16	85 40	741 65	577 99
8	1 271 04	97 60	847 60	660 56
9	1 429 92	109 80	953 55	743 13
10	1 588 80	122 00	1 059 50	825 70
11	1 747 68	134 20	1 165 45	908 27
12	1 906 56	146 40	1 271 40	990 84
13	2 065 44	158 60	1 377 35	1 073 41

FIG. 1—*Table of multiples of star constants* (1950) *for the right ascension of No.* 1073 (268 *G. Ceti*).

7. *Initial settings.*—The final stage of the preparatory work is the calculation of initial setting values, and a check value, for the National machine. The setting values, which are here listed in the order in which they are required to be set, are calculated from the following formulae:

$$\left.\begin{aligned} \delta^3_{-15} &= x \\ \alpha_{-10} &= u + rv + G_{-10} \\ \Delta_{-15} &= \tfrac{1}{2}v - (\tfrac{1}{2} - 2r)w - rx + g \\ \delta^2_{-10} &= w \\ r\delta^3_{-15} &= rx \end{aligned}\right\} \qquad (16)$$

and the check value, which should be reproduced within a few hundred in the end figure (that is, within about 3×10^{-3} of the published unit), is

$$\alpha_{\text{check}} = y + rz + G_{\text{check}} \qquad (17)$$

In these expressions u, v, w, x, y, z are the sums of the products of U, V, W, X, Y, Z by their corresponding star constants. An example of this calculation is given below for the right ascension of 268 G. Ceti, for which the corresponding star constants have been tabulated in Fig. 1.

268 G. Ceti (No. 1073)

α_0	$2^h\ 33^m\ 20^s{\cdot}105$		α_0	$2^h{\cdot}56$	
μ_α	$+0{\cdot}1210$		r	$-0{\cdot}0197$	
$e\psi$	$+0{\cdot}00768$		$\frac{1}{2}-2r$	$+0{\cdot}5394$	
a	$+3{\cdot}1699$				
$\mu_\alpha - e\psi$	$+0{\cdot}11332$	τ_{-10}	$-0{\cdot}02756$	τ_{380}	$+1{\cdot}03731$
$a + e\psi$	$+3{\cdot}17758$	$2A_{-10}$	$-0{\cdot}2027$	$2A_{380}$	$+2{\cdot}2058$

G_{-10}	$20{\cdot}102\ 40000$				
		g	$+0{\cdot}003\ 09297$		
G_{380}	$20{\cdot}223\ 02591$			G_{check}	$20{\cdot}223\ 02583$

u	$+\ 475\ 70270$	δ^3_{-15}	$4\ 149\ 74$
v	$-\ 98\ 17457$	α_{-10}	$20{\cdot}580\ 036\ 74$
w	$-\ 28\ 83003$	Δ_{-15}	$999{\cdot}969\ 638\ 35$
x	$+\ 4\ 14974$	δ^2_{-10}	$999{\cdot}971\ 169\ 97$
		$r\delta^3_{-15}$	$999{\cdot}999\ 918\ 25$
y	$+3{\cdot}819\ 01489$		
z	$-\ 212\ 52464$	α_{check}	$24{\cdot}046\ 227\ 46$

8. *National set-up.*—The "set-up" on the National machine is illustrated in Fig. 2, which is a direct reproduction of the standard form used in the Nautical Almanac Office. It gives details of the stops used, the operations (setting and register selection) and the various quantities printed at the different stages in each cycle; as an instruction sheet to the operator of the machine it also gives all necessary operating details.

Although the set-up appears complicated, it is essentially a simple mechanization of (12), (13) and (14) of Section 4. The general principle consists of building up δ^2 from the pre-computed δ^4 in the obvious way, and then α and Δ from δ^2 and multiples of δ^3; by using the otherwise empty register 2, $r\delta^3$, which enters into two values of Δ, need only be set once. For the practical purpose of producing the final values in a form directly suitable for use as printer's copy, the function (correctly rounded off and treated as positive in all cases) and the *following* difference Δ (in its direct form, whatever its sign) must be printed in that order. This is achieved by building up Δ and the modulus of Δ in two separate registers, one being the subtracting register 1, using (12) in precisely the form given.

It will be noticed that the last two positions of the normal cycle (positions 12 and 13) produce printer's copy, with the exception that the first difference printed is the non-rounded-off difference of the non-rounded-off function values instead of the true difference of the rounded-off values. It is possible, by one additional setting on each line, to produce the actual difference required, but it is much better

NATIONAL SET-UP FOR
APPARENT PLACES OF STARS (10-DAY COPY)

Group No. APS/3

Serial No. 49

(from Besselian Day Numbers at 12^h G.S.T.)

Position	0	1	2	3	4	5	6	7	8	9	10	11	12	13	14	15	16
Stop	M	0	±3	±3	±3	±3	$5,\pm1$	0	$6,\pm1$	$6,\pm1$	4	$2,6,\pm1$	0 $(\frac{1}{2}NP)$	-1 $[\frac{1}{2}NP]$	0,R	2	R
Operation	-	Set	Set	Set	Set	Set	ST6	ST5	T2	ST4	ST3	Set	ST5	ST1	-	-	-
Print	-	$Arg._n$	Four fourth differences δ_n^4				Δ_{n-5}	a_n	$r\delta_{n-5}^3$	δ_n^2	δ_{n+5}^3	$+r\delta_{n+5}^3$	a_n	$\pm\Delta_{n+5}$	-	-	-
Initial Set-up	(i) -		Set δ_{-15}^3	on +3			Set a_{-10}	T1	Set Δ_{-15}	-	Set δ_{-10}^2	-	-	-	-	Set $r\delta_{-15}^3$	-
	(ii) Set $Arg._{-10}$	-	-	-	-	-	-	-	T2	ST4	ST3	Set $r\delta_{-5}^3$	-	ST1	-	-	-
	Normal operation will produce the next line (i.e. line 0).																
Set-up from completed line	(i) -		Set δ_{n+5}^3	on +3			Set a_n	T1	Set Δ_{n-5}	-	Set δ_n^2	-	-	-	-	Set $r\delta_{n-5}^3$	-
	(ii) Set $Arg._n$	-	-	-	-	-	-	-	T2	ST4	ST3	Set $r\delta_{n+5}^3$	ST5	ST1	-	-	-
	Normal operation will produce the next line (i.e. line n + 10).																

INITIAL SETTINGS

These are taken from the working sheets in the form required.

SIGNS OF STOPS

Pos.	Stop	Sign
2	±3	Same as $a \times \delta^4$ (A)
3	±3	Same as $b \times \delta^4$ (B)
4	±3	Same as $c \times \delta^4$ (C)
5	±3	Same as $d \times \delta^4$ (D)
6	$5,\pm1$	Same as Δ
8	$6,\pm1$	Same as Δ
9	$6,\pm1$	Same as Δ
11	$2,6,\pm1$	Same as Δ

PRINTING. For R.A. (declination less than 60°), print in banks 2 to 11 inclusive and adjust $\frac{1}{2}NP$ to cut off 6 figures; otherwise print in banks 3 to 12 with $\frac{1}{2}NP$ cutting off 7 figures.

SPACING. Single spacing with normal blocks of five is to be used.

HEADINGS. Set Star No. in positions 1, 7 and 12; two lines down set the year in position 1 and the hours (or degrees) and minutes in position 12. The next two lines will then comprise the initial set-up.

SETTINGS. Those in positions 2 to 5 are taken from the table of multiples of the star constants, determined by the tabular fourth differences of the corresponding Day Numbers; the signs of the stops must be carefully checked initially and thereafter reversed whenever the corresponding δ^4 changes sign. The setting in position 11 is obtained by rounding off the product of the constant r by δ^3 just printed in position 10, all quantities being here treated as complements if negative.

FIRST DIFFERENCE. Immediately before a change of sign, reverse the stops in positions 6, 8, 9 and 11.

CHECK. The function on line 380 should not differ by more than 260 from the MS. check provided.

FIG. 2.—*National "set-up" for the computation and preparation of printer's copy for the apparent places of 10-day stars.*

NATIONAL SET-UP FOR

APPARENT PLACES OF STARS (10-DAY COPY)

(from Besselian Day Numbers at 12^h G.S.T.).

Group No. APS/3

Serial No. 49

Position	0	1	2	3	4	5	6	7	8	9	10	11	12	13	14	15	16
Stop	M	0	±3	±3	±3	±3	5,±1	0	6,±1	6,±1	4	2,6,±1	0 ($\frac{1}{2}$NP)	-1 [$\frac{1}{2}$NP]	0,R	2	R
Operation	-	Set	Set	Set	Set	Set	ST6	ST5	T2	ST4	ST3	Set	ST5	ST1	-	-	-
Print	-	Arg.n	Four fourth differences δ_n^4				Δ_{n-5}	a_n	$r\delta_{n-5}^3$	δ_n^2	δ_{n+5}^3	$+r\delta_{n+5}^3$	a_n	$\pm\Delta_{n+5}$	-	-	-
Initial Set-up	(i) -		Set δ_{-15}^3	on +3			Set a_{-10}	T1	Set Δ_{-15}	-	Set δ_{-10}^2	-	-	-	-	Set $r\delta_{-15}^3$	-
	(ii) Set Arg.$_{-10}$	-	-	-	-	-	-	-	T2	ST4	ST3	Set $r\delta_{-5}^3$	-	ST1	-	-	-
	Normal operation will produce the next line (i.e. line 0).																
Set-up from completed line	(i) -		Set δ_{n+5}^3	on +3			Set a_n	T1	Set Δ_{n-5}	-	Set δ_n^2	-	-	-	-	Set $r\delta_{n-5}^3$	-
	(ii) Set Arg.n	-	-	-	-	-	-	-	T2	ST4	ST3	Set $r\delta_{n+5}^3$	ST5	ST1	-	-	-
	Normal operation will produce the next line (i.e. line n + 10).																

INITIAL SETTINGS

These are taken from the working sheets in the form required.

SIGNS OF STOPS

Pos.	Stop	Sign
2	±3	Same as $a \times \delta^4$ (A)
3	±3	Same as $b \times \delta^4$ (B)
4	±3	Same as $c \times \delta^4$ (C)
5	±3	Same as $d \times \delta^4$ (D)
6	5,±1	Same as Δ
8	6,±1	Same as Δ
9	6,±1	Same as Δ
11	2,6,±1	Same as Δ

PRINTING. For R.A. (declination less than 60°), print in banks 2 to 11 inclusive and adjust $\frac{1}{2}$NP to cut off 6 figures; otherwise print in banks 3 to 12 with $\frac{1}{2}$NP cutting off 7 figures.

SPACING. Single spacing with normal blocks of five is to be used.

HEADINGS. Set Star No. in positions 1, 7 and 12; two lines down set the year in position 1 and the hours (or degrees) and minutes in position 12. The next two lines will then comprise the initial set-up.

SETTINGS. Those in positions 2 to 5 are taken from the table of multiples of the star constants, determined by the tabular fourth differences of the corresponding Day Numbers; the signs of the stops must be carefully checked initially and thereafter reversed whenever the corresponding δ^4 changes sign. The setting in position 11 is obtained by rounding off the product of the constant r by δ^3 just printed in position 10, all quantities being here treated as complements if negative.

FIRST DIFFERENCE. Immediately before a change of sign, reverse the stops in positions 6, 8, 9 and 11.

CHECK. The function on line 380 should not differ by more than 260 from the MS. check provided.

FIG. 2.—*National "set-up" for the computation and preparation of printer's copy for the apparent places of 10-day stars.*

to make the necessary amendments by hand than to add a further complication to the set-up. The last two columns are actually torn off and pasted, with the corresponding columns for the declination and other stars, to form the copy sent to the printer.

No further details of the set-up need be given here; if such are required it is suggested that the contents of each register be traced through one or two cycles.

9. *Operation and example.*—It is of interest to follow through in some detail the actual operations required, and for this purpose reference will be made to the example illustrated in Fig. 3; this is a reproduction (slightly reduced) of the actual sheet printed by the National machine in producing the right ascension of 268 G. Ceti. Normally, the only writing on the sheet will be the end-figure alterations to the first difference, but here explanatory headings and checks have been written in to assist interpretation. The initial settings are available in precisely the form required (see Section 7) and are set into the machine in the positions indicated on the set-up; $r\delta^3_{-15}$ is not recorded when set, as position 15 is off the paper, but it is printed in position 8 on line −10. The first line (−10) is rather special, but line 0 is normal, apart from the fact that the fourth differences are all zero. Let us follow through a normal cycle, say line 20; the successive operations to be carried out are the following:

(i) Set the argument, 20, in position 1.

(ii) Set the four fourth differences in positions 2–5, the signs of the corresponding stops being correctly set; each is that multiple of the appropriate star constant (Fig. 1) indicated by the fourth difference of the corresponding Day Number (Table I).

Thus:

	A	*B*	*C*	*D*
from Table I	+9	+2	−9	+9
from Fig. 1	+1 429 92	+24 40	−953 55	+743 13

It should be noted that the star constants are here all positive, but this need not be the case.

(iii) Operate the machine, as indicated in the set-up, in positions 6–10, printing $\delta^3_{25} = 6\ 268\ 14$ in the last of these positions.

(iv) Calculate $r\delta^3_{25}$ and set it in position 11. The calculation is done on an auxiliary calculating machine (actually a Marchant automatic electric machine, model ACT 10M, is used), on the keyboard of which r (in complementary form if negative and thus here 9999 999 803) is set; the multiplier is δ^3_{25} (in complementary form if negative) exactly as printed in position 10. Here it is in direct form and the rounded-off product, 99 999 876 52, which is set in position 11, is copied from the product register of the machine which actually reads *6268139* 876 51 *7642*.

(v) Operate the machine in positions 12 and 13.

The carriage then returns automatically to position 1 and the cycle recurs on line 30.

In addition to this routine, the operator has to watch the sign of Δ and *anticipate* a change, as well as seeing that the printed values do not indicate any gross error.

In due course line 380 is reached and α_{380} (here 24 046 227 98) printed; this is compared with the check value (24 046 227 46) previously computed. If the discrepancy (here 52) does not exceed 260 (it has a standard deviation of 79), it is attributed to the accumulation of rounding-off errors arising from the terms $r\delta^3$;

apart from these terms there should, of course, be exact agreement. Any real error is likely to give rise to a much larger discrepancy. Any such discrepancy must be explained and the computation either re-done *ab initio*, or, if the error occurs towards the end of the tabulation, corrected by setting up from a completed correct line.

10. *Discussion.*—In the previous Section it is seen that the operator has to make nearly 200 settings on the keyboard of the National machine, 39 of these being the results of multiplications on the auxiliary machine, as well as setting arguments and selecting registers. The average time taken for all this is 20–25 minutes (it has been done in 15 minutes!) and the number of cases in which the check fails (and it will fail if a single error is made!) is less than 20 per cent. In many of these only a portion of the computation needs to be re-done, while even the complete recomputation can be done much more quickly than the original. Errors are not usually difficult to trace and are often due to the setting of erroneous multiples in δ^4, leading to large discrepancies. On the whole, therefore, 30 minutes is an adequate estimate for a single correct computation. The calculation of the star constants (done once every ten years), the setting values and the correction of the end figures of Δ (on the average half the end figures of Δ must be increased by unity) do not take more than 20 minutes for each coordinate. Actually, a completely independent check is also made to guard against systematic errors, but this, which is common to all methods, is not included in these times. Copy, completely checked and printed in perfect form for the printer, can thus be prepared at an average time of about $1\frac{1}{2}$ hours for each star. This compares very favourably with other methods.

11. *Acknowledgments.*—The authors are indebted to Mr A. E. Carter for the final form of the National set-up and for valued assistance at all stages of the development of the method; they are grateful in no small measure to the National operators, in particular Miss D. M. Fooks and Miss Y. I. Reddy, whose speed and accuracy have made the method possible.

H.M. Nautical Almanac Office, Bath:
1948 *January* 3.

Reference

(1) L. J. Comrie, *Supplement to the Journal of the Royal Statistical Society*, Vol. III, 87, 1936.

CHROMOSPHERIC FLARES

R. G. Giovanelli

(Received 1948 March 10)

Summary

A brief account of the observed properties of chromospheric flares is followed by a theory of their origin. This theory involves electric fields produced by variations in the magnetic flux through a nearby sunspot, as discussed in a previous paper. If the electric field exceeds a certain value, then electrons acquire sufficient energy to excite hydrogen atoms at collisions, and flares may result.

The theory shows that flares should occur in specific locations, which depend largely on the configuration of the magnetic field, in the neighbourhood of spot groups. The majority of the well-known features of flares, including their occurrence in the chromosphere, their stationary nature, their sudden beginning, and their correlation with the rate of growth of spots, are accounted for, and the theory also accounts for the amount of radiation emitted.

---

1. *Introduction.*—The occurrence of chromospheric flares has long been recognized as a striking feature of solar activity, especially in view of the close association of flares with many terrestrial phenomena, such as radio fadeouts, magnetic storms and auroras.

In this paper some of the known properties of flares are reviewed briefly, and a theory is presented to explain the majority of these features.

2. *Properties of Chromospheric Flares.*—The term chromospheric flare is given to the localized, large and sudden increase in certain monochromatic radiations emitted from the solar chromosphere. The radiations in which the greatest increases are observed consist mainly of the H and K lines of ionized calcium and the $H\alpha$ line of hydrogen, although smaller increases in the emission of many other lines of these and other elements have been observed (1).

During the past ten years intensive observation has established many facts concerning flares. They are essentially short-lived phenomena, lasting from a few minutes to an hour or more, the average life being of the order of 30 minutes (2), and the maximum brightness occurring after an average time of seven minutes (3, 4). The beginning of a flare is remarkably sudden and may be timed, if observed, to within less than a minute.

Flares almost invariably occur in the neighbourhood of a sunspot group. An analysis of the solar flares listed in the *Bulletin for Character Figures of Solar Phenomena* for 1935–1937 has led to the conclusion (5) that the probability of a flare occurring in the neighbourhood of a sunspot group is, other things being equal, proportional to the area of the group, although the factor of proportionality is different for different types of spot groups. For groups of the same size the probability that a flare will occur in the neighbourhood of the group is least for the unipolar α groups, a little greater for the β, βf and βp groups, somewhat greater still for the more complicated $\beta\gamma$ groups, and very much greater for the complex γ groups. Moreover, for groups of the same type the probability of occurrence, per unit area of the spot group, depends on the rate of change of area, being greater for a growing spot or for one which is just disappearing from the surface of the

Sun than for one which is otherwise decreasing or of constant area. For a given size of spot group the probability is not directly dependent on the maximum value of the magnetic field in the group.

As a result of a large number of observations of the wave-length of the $H\alpha$ emission line it has now been established that the emitting atoms have no vertical drift velocity (**3**, **4**, **6**) to within the limits of observational error, i. e. to within one or two km./sec. Ellison (**3**) has shown that there is no lateral movement of a flare, although a slow diffusion and spreading of the emitting region may be observed once the greatest intensity is passed.

It has been generally accepted that flares are in the main confined to the chromosphere, although Allen (**1**) has shown that there is a detectable change in the relative intensities of Fraunhofer lines below the flare, and the author has observed one flare (**7**) in a prominence on the limb.

The $H\alpha$ line radiated from the flare is slightly reversed in the centre (**3**) and may have a central intensity between 50 per cent and 150 per cent of that of the surrounding continuous spectrum (**4**). The total width of the emission line lies between 1·75 and 4 angstrom units, although in the majority of cases the widths are close to the former value (**4**).

The area covered by a flare may range from less than 100 to over 1000 millionths of the Sun's disk. No analysis has been published concerning the shapes of flares, but the author was repeatedly impressed during observations in the period 1937–1939 by their fairly sharply-defined appearance. A large number occurred in the form of a filament of width about 2000 km. Near a unipolar spot such a flare sometimes formed a rather small arc of a circle concentric with the spot, but for bipolar and more complex groups the lines were much more irregular. The majority of the flares did not pass immediately over a spot. Ellison (**3**) has also pointed out that the really great flares frequently have the form of brilliant ropes or filaments many times greater in length than breadth.

In a note on "A Theory of Chromospheric Flares" (**8**) it was shown that the induced electric fields due to the changing magnetic flux of a sunspot will set up currents in the neighbourhood of the sunspot. The conductivity of the chromosphere is low in a direction perpendicular to the magnetic field when its field strength exceeds a value of the order of a gauss, and the current flows only along the lines of magnetic force. A complete circuit around the spot is possible if this current passes through a neutral point in the magnetic field. The current follows lines of magnetic force from near the neutral point down into the Sun where the high electron pressure allows of high electrical conductivity across the magnetic field. It was pointed out that if electrons collide mainly with atoms, having fixed collision radii, neutral hydrogen atoms would be excited at collisions with electrons if the mean free path of the latter exceeds $4{\cdot}5 \times 10^7/E$ cm., E being the electric field measured in e.m.u. This condition is satisfied at times in the chromosphere.

The simple theory summarized above requires elaboration. A more detailed theory, in which it is assumed that low energy electrons collide mainly with protons, and which accounts for the major features of chromospheric flares, will now be given.

3. *Electron Energies in an Electric Field.*—Except perhaps in its very lowest layers, the chromosphere is a highly ionized gas in which the electron energy in the presence of a weak electric field is limited by energy losses due to elastic collisions

with positive ions. The mean free path between these collisions increases rapidly as the electron energy increases.

The rate of gain of energy of an electron in crossed electric and magnetic fields has been discussed by the author elsewhere (**9**). For an electron of energy W, less than the excitation potential of any neutral atoms, the rate of gain of energy is given approximately by

$$\frac{dW}{dt} = \frac{E^2c^2u^2}{\pi\beta^2 mN_+Z^2(1+e^2H^2u^6/\pi^2\beta^4N_+^2m^2Z^4)} - \frac{\pi\beta^2m^2N_+Z^2}{Mu}\left(1-\frac{u_0^2}{u^2}\right),$$

where e, m and u are the electron charge, mass and velocity in e.m.u. and c.g.s. units, c the velocity of light, M the mass of a positive ion, Z the mean degree of ionization (which may be taken as unity), E and H the electric and magnetic field strengths (e.m.u.), N_+ the positive ion concentration (assumed equal to the electron concentration), u_0 the mean velocity of electrons in thermodynamic equilibrium with the positive ions and β a constant equal to $1{\cdot}57 \times 10^9$ cm.^{3} sec.$^{-2}$.

If the electric field be parallel to the magnetic field, or if H be zero, dW/dt is positive for u large compared with u_0, and the electron energy is not limited by collisions with positive ions. It was shown (**9**) that for any given value of u_0 there exists a critical value of the electric field strength below which the electron energies are stable and above which the electron energy is not limited by collisions with positive ions, so that in the absence of inelastic collisions the electron energy will increase to limits imposed only by the extent of the field. The value, E_c, of the critical field strength is given by

$$E_c = \frac{2\sqrt{3}}{9} \cdot \frac{\pi\beta^2 m^{\frac{1}{2}}N_+Z^2}{u_0^2 eM^{\frac{1}{2}}}.$$

The value of the critical field falls as the energy of the positive ions increases. This energy increases in the presence of an electric field, but much more slowly than the energy of the electrons. There is insufficient data to calculate the rate of loss of energy of the ions, and hence to calculate the increase in energy above the normal, which we assume corresponds to 5750 deg. K. With hydrogen ions at this temperature, the critical field has the value

$$E_c = 1{\cdot}51 \times 10^{-6}N_+ \text{ e.m.u.}$$
$$= 2{\cdot}0 \times 10^6 p \text{ e.m.u.},$$

where p is the pressure of the positive ions in dynes/cm.^{2}.

It may be shown that while the electron energy remains in an equilibrium state it does not exceed 1·5 times the thermal energy of the ions.

In the chromosphere the ionization of any gas is incomplete, but it has been pointed out by Cowling (**10**) that under normal conditions collisions are mainly with ions. If elastic collisions at thermal velocities occur mainly with ions they may be expected to occur mainly with ions at considerably higher velocities. If the magnitude of the electric field be such that elastic collisions cannot limit the electron energy, the only effective slowing-down processes can be those involving excitation or ionization which, however, cannot take place until the electron energy at least equals the excitation energy.

As will be shown in another paper, there is a second critical field, E_L, such that when $E < E_L$ electron energies will not greatly exceed the excitation potential but when $E > E_L$ electron energies cannot be limited by excitations. Assuming

inelastic collisions to occur only with hydrogen atoms of concentration N per c.c., of excitation potential 10·1 e.V., and of assumed collision radius 10^{-8} cm., then

$$E_L = 2{\cdot}0 \times 10^{-6}\{N(N_+ + N/5)\}^{\frac{1}{2}} \text{ e.m.u.}$$

While the concentration of neutral and ionized atoms may be very different in flares from those in the normal chromosphere, the proton concentration, N_+, will be assumed equal to the normal electron concentration n given by Cillié and Menzel (**11**) as

$$n = 3{\cdot}9 \times 10^{11} \exp(-0{\cdot}77 \times 10^{-8}x) \text{ per c.c.},$$

where x is the height, in cm., above the base of the chromosphere. The concentration of neutral hydrogen atoms is very uncertain, but will be assumed to be

$$N = 2{\cdot}6 \times 10^{13} \exp(-1{\cdot}54 \times 10^{-8}x) \text{ per c.c.},$$

using Cillié and Menzel's data for hydrogen atoms in the 2-quantum state and an excitation temperature of 4740 deg. K. Then it is found that E_L exceeds E_c when x is less than 6000 km., i. e. throughout the lower chromosphere.

The critical fields and the neutral and ionized hydrogen atom concentrations are given in Table I.

TABLE I

Concentration, Pressure and Critical Fields for the Chromosphere

Height above base of chromosphere	Electron concentration $n(=N_+)$	Neutral hydrogen atom concentration	Electron pressure	E_c (elastic collisions with ions)	E_L (excitation of neutral hydrogen atoms)
10^3 km.	per c.c.	per c.c.	dyne/cm.^{2}	e.m.u.	e.m.u.
0	$3{\cdot}9\times10^{11}$	$2{\cdot}6\times10^{13}$	$3{\cdot}0\times10^{-1}$	$5{\cdot}9\times10^{5}$	$2{\cdot}4\times10^{7}$
1	$1{\cdot}8\times10^{11}$	$5{\cdot}6\times10^{12}$	$1{\cdot}4\times10^{-1}$	$2{\cdot}7\times10^{5}$	$5{\cdot}4\times10^{6}$
2	$8{\cdot}4\times10^{10}$	$1{\cdot}2\times10^{12}$	$6{\cdot}3\times10^{-2}$	$1{\cdot}3\times10^{5}$	$1{\cdot}2\times10^{6}$
3	$3{\cdot}9\times10^{10}$	$2{\cdot}6\times10^{11}$	$3{\cdot}0\times10^{-2}$	$5{\cdot}8\times10^{4}$	$3{\cdot}1\times10^{5}$
4	$1{\cdot}8\times10^{10}$	$5{\cdot}5\times10^{10}$	$1{\cdot}4\times10^{-2}$	$2{\cdot}7\times10^{4}$	$8{\cdot}0\times10^{4}$
5	$8{\cdot}3\times10^{9}$	$1{\cdot}2\times10^{10}$	$6{\cdot}2\times10^{-3}$	$1{\cdot}3\times10^{4}$	$2{\cdot}3\times10^{4}$

The theory of the critical field has neglected the distribution of electron velocities and free paths about their means. With fields below the computed critical field, some electrons, having energies well above the mean, can be accelerated to high energies. If we assume that on reaching the excitation potential of any neutral atoms present the electrons lose most of their energy, then corresponding to any electric field there will be a mean electron energy which increases rapidly but continuously with field strength when the latter approaches E_c. Associated with this process there will be an accompanying emission of radiation which we proceed to identify with that of a flare.

The simple theory of the critical field predicts a sudden increase in the current density when the electric field reaches E_c. For a typical case, in which electrons lose energy on reaching the excitation potential, the conductivity was found to increase by a factor of four. This discontinuity would be replaced in a statistical theory by a continuous but nevertheless rapid increase in conductivity when the field strength approaches E_c.

4. *Electric Fields Around Growing Sunspots.*—The variation in magnetic flux from a sunspot sets up in the Sun's atmosphere an electric field, the configuration and magnitude of which depend on the conductivity of the atmosphere.

A discussion of the fields in a bipolar group whose axis is perpendicular to the Sun's general field has been given previously (**12**) for the simple case of two sunspots which are relatively weak and far apart so that no lines of force extend directly from one sunspot to the other but are absorbed by the Sun's general magnetic field. The essential results are summarized below.

Beneath the Sun's surface the conductivity is so high that the velocity of propagation of a magnetic field is only of the order of 80 km./day. In the atmosphere the rate of propagation would also be very low but for the low conductivity perpendicular to a magnetic field of strength greater than about one gauss.

The Sun's general magnetic field, and that due to other sunspots, combines with the sunspots' magnetic fields, giving rise to lines of force as shown in Fig. 1. When the magnetic flux from a sunspot changes, the induced current is effectively directed along lines of magnetic force except near the neutral point. The current system depends, however, on the manner of creation of the sunspots, i.e. the way in which the lines of magnetic force break out into the atmosphere. It is not material to our argument just what mechanism is assumed, but we will adopt Alfvén's model (**13**) in which a sub-surface toroidal magnetic field breaks through the surface of the Sun. At least two types of current system can occur in the atmosphere (see Fig 1). In the first, the current flows in a sheet towards and through the neutral point. In the second it flows into or out from a sunspot.

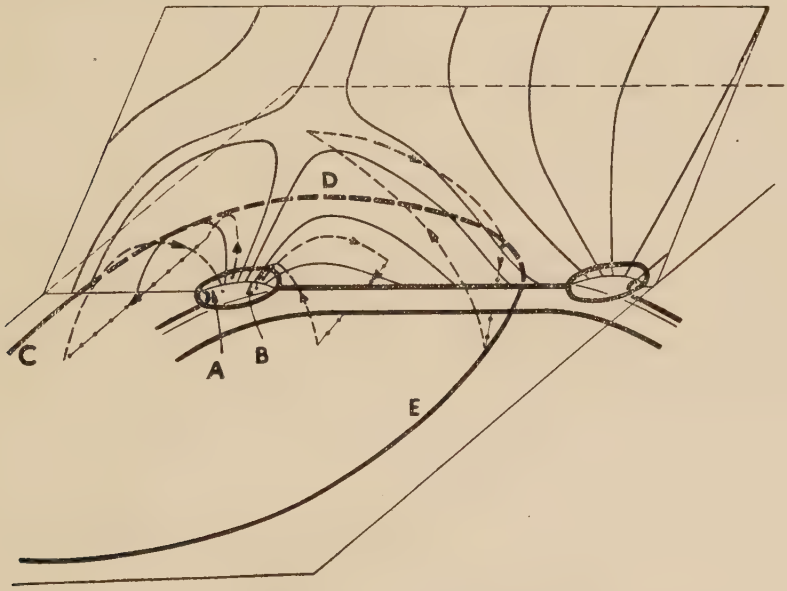

FIG. 1.—*Currents near a growing bipolar spot group.*

Lines of magnetic force are shown in a plane (the "dividing" plane) containing the Sun's general magnetic field, and intersecting the two sunspots. Typical current filaments (1) in the neutral point current sheet and (2) flowing into sunspots, are indicated by broken lines, and their relative directions given. The line AB is the locus of points where the dividing plane meets the surface of the sunspot, so that lines of force from AB eventually return to the Sun along the axis of the spot group. CDE is the locus of points where lines of force from near the neutral point meet the Sun's surface and is thus the base of the neutral point current sheet.

If anywhere along the above circuits the electric field approaches E_c, flares may occur, and we shall now discuss their locations.

5. *Flares on Current Paths passing through a Neutral Point.*—Because of the finite time of propagation of the electromagnetic field, the maximum current density (and thus the maximum electric field) in the first current system occurs along lines of magnetic force which meet the Sun's surface near the sub-surface toroid. Thus in a simple bipolar group consisting of two equal sunspots, with a general magnetic field perpendicular to the axis of the group and inclined to the Sun's surface, there will be a maximum current density close to the plane containing the general field and spot-group axis. This plane, which we shall call the dividing plane, also contains the neutral point.

It is difficult to estimate satisfactorily the electric field near the neutral point. A lower limit may be obtained, however, by regarding lines of magnetic force as perfectly insulated conductors when $H/p>2$, the conductivity being unaffected by the magnetic field when $H/p<2$ (p being the electron pressure). On this basis it was shown (**12**) that the current at the neutral point has a cross-sectional area of the order of $2a_n^2p^2/3G^2$, where a_n is the distance of the neutral point from the sunspot, G the strength of the constant external magnetic field and p the electron pressure at the neutral point. Putting $a_n=3{\cdot}5\times10^9$ cm. and $G=25$ gauss, the area is $1{\cdot}7\times10^{16}p^2$ cm.^{2}.

It has also been shown (**12**) that if the field can be propagated rapidly through the atmosphere, so that in the neutral point current sheet the current on one side of the dividing plane flows towards the neutral point from all directions, then the current density near the neutral point is roughly $1{\cdot}7\times10^{-3}p$ e.m.u. for a typical sunspot which has a final central magnetic field H_0 of 2000 gauss and a final radius of 7×10^8 cm., while the flux from it increases as $B\sin\omega t$, where $\omega=5{\cdot}6\times10^{-6}$ sec.$^{-1}$ (i.e. it reaches maximum size in 78 hours). For a conductivity of 10^{-8} e.m.u. the corresponding electric field is $1{\cdot}7\times10^5p$ e.m.u. Consideration of the finite rate of propagation would have led to a lower computed field.

On our simple theory involving zero conductivity perpendicular to an appreciable magnetic field, the cross-section of the current path is a maximum, and hence the electric field a minimum, near the neutral point. Fuller consideration of the conductivity at right angles to the magnetic field would lead to a much increased electric field at the neutral point.

The computed field, as given above, is approximately one-fifteenth of the critical field. But this is based on a maximum rate of sunspot growth of about 25 millionths of the Sun's hemispherical surface per day. Rates of growth of many times this are, however, quite normal. Thus we may expect that near the neutral point there are at times electric fields exceeding the critical field. As all current paths pass through this region it is a likely location for flares.

At a point on the current sheet where the radius from the sunspot makes an angle θ with the line joining the sunspot and neutral point, the current sheet has a thickness t where, if the conductivity at right angles to the magnetic field be zero for $H/p>2$,

$$t=(2/3)^{\frac{3}{2}}(p/G)^3a_n/(\sin\theta\,.\,\sin\tfrac{1}{2}\theta)\text{ cm., approximately (12),}$$

or

$$t=1{\cdot}2\times10^6p^3/(\sin\theta\,.\,\sin\tfrac{1}{2}\theta)\text{ cm.}$$

Thus the current sheet is very thin except near the neutral point, so that it is doubtful whether, looking normally on to the surface, an increased emission there could be observed. At a grazing angle, however, the increase in brightness will

be much greater, and a flare may be observable if the current sheet close to the dividing plane is seen tangentially. Such a flare would appear as an arc roughly concentric with the sunspot, as shown in Fig. 2.

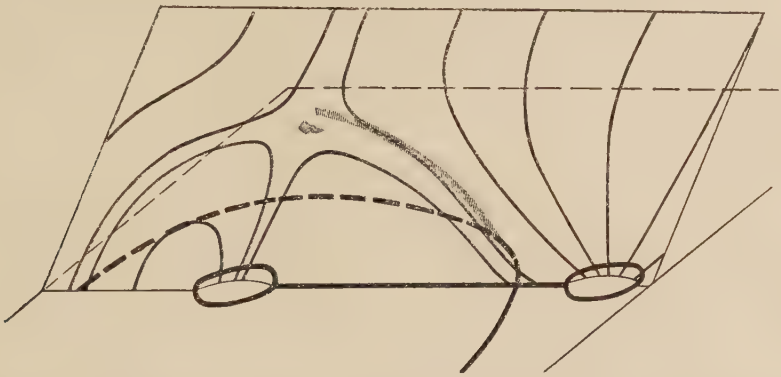

FIG. 2.—*Neutral point flare.*

Some possible locations for neutral point flares are shown hatched in the above figure. The isolated area is in the neighbourhood of the neutral point; the long arc represents a tangential view of the neutral point current sheet. A flare may occupy part of the region shown.

6. *Flares on Current Paths passing into a Sunspot.*—The currents that pass into sunspots are volume currents, and they flow into the spot on one side of the dividing plane and outwards on the other side (see Fig. 1). The magnitude of the current depends largely on the resistance of the sunspot, and this is uncertain. It is convenient to discuss the resistance of the current filament within the sunspot in terms of the length s of a cylindrical conductor of constant conductivity $\sigma = 10^{-8}$ e.m.u. (the same as the chromosphere in the absence of a magnetic field), having constant cross-section equal to that of the current filament at the surface of the spot, and having the same resistance as the current filament within the sunspot. For filaments entering close to the dividing plane or near the edge of the sunspot, s is smaller than for other filaments. Moreover, the e.m.f. is a maximum around circuits lying close to the dividing plane, so that the component of the electric field strength in the direction of the magnetic field should be a maximum close to this plane. Along lines of magnetic force which return to the Sun between the two sunspots and close to the dividing plane, the electric field in the direction of the lines of magnetic force is given roughly by (12)

$$E = 6 \times 10^{25}/a^2(18 + 2{\cdot}9 \times 10^{-8}s) \text{ e.m.u.}$$

for the sunspot data assumed earlier, a being the distance of the point considered from the sunspot.

It has been shown that the magnetic field can grow rapidly along the dividing plane, but at right angles to this plane the rate of propagation is a function of the sunspot resistance. The concept of a velocity of propagation is useful, provided it is not interpreted too rigidly, for the wave-form of the disturbance changes markedly with distance. Table II summarizes results obtained previously (12). For a

TABLE II

Electric Fields along Circuits through Sunspots

s (cm.)	10^7	10^8	10^9	10^{10}	10^{11}	10^{12}	10^{13}
Penetration velocity $\times r^{\frac{1}{2}}$ (cm.$^{\frac{3}{2}}$/sec.)	$3{\cdot}3 \times 10^6$	$3{\cdot}6 \times 10^6$	$5{\cdot}4 \times 10^6$	$1{\cdot}4 \times 10^7$	$4{\cdot}3 \times 10^7$	$1{\cdot}4 \times 10^8$	$4{\cdot}3 \times 10^8$
E (e.m.u.)	$2{\cdot}7 \times 10^5$	$2{\cdot}3 \times 10^5$	$1{\cdot}0 \times 10^5$	$1{\cdot}6 \times 10^4$	$1{\cdot}7 \times 10^3$	$1{\cdot}7 \times 10^2$	$1{\cdot}7 \times 10$

given value of s, there are tabulated both the corresponding value of the velocity of penetration of the magnetic field at a distance r from the axis of the spot group and the electric field strength in the direction of the lines of magnetic force. These are given in this table for the sunspot data used before, E being computed for a distance $3{\cdot}5 \times 10^9$ cm. from the sunspot. Roughly, E is inversely proportional to the square of the distance from the sunspot, so that near the edge of the sunspot ($3{\cdot}5 \times 10^8$ cm. from the centre) it will be about 100 times as great as tabulated.

If we consider a point where the electron pressure is 0·01 dyne/cm.^{2}, E_c is $2{\cdot}6 \times 10^4$ e.m.u. There will be regions determined by the rate of propagation of the field where E can be of this magnitude. For example, changes in the field are propagated outwards at a velocity V which varies with the distance r. For a given sunspot resistance, the distance from the spot-group axis to which the changes in field will have been propagated is of the order of magnitude of Vt, where V is the velocity at the distance reached. Thus, from Table II, if $t = 10^5$ sec. and $s = 10^{11}$ cm., the distance r to which the field has been propagated is of the order of $2{\cdot}5 \times 10^8$ cm. If we now consider such a path, E exceeds $2{\cdot}6 \times 10^4$ e.m.u. as far as 9×10^8 cm. from the sunspot provided the path lies within $2{\cdot}5 \times 10^8$ cm. from the spot-group axis. The field may exceed E_c only at parts of any current filament, however, for the current paths are inclined to the Sun's surface and E_c decreases with height. Thus we see that there are two factors which limit the extent of a flare:

(*a*) The velocity of propagation of the magnetic field;

(*b*) The relation between the variation of E and the variation of E_c with distance from the sunspot.

In general it may happen that (i) the value of s is so small for current filaments close to the dividing plane that flares are confined to its immediate neighbourhood; or (ii) s is effectively constant for all conducting tubes and of such magnitude that flares can occur over a region whose width depends solely on the penetration velocity; or (iii) s is large enough to allow flares to occur over a considerable distance from the dividing plane, whereas for filaments further out s becomes so large as to reduce E below E_c; or (iv) s is too large for flares to occur anywhere.

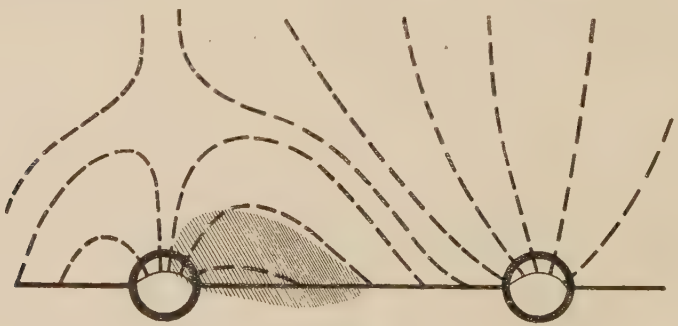

FIG. 3.—"*Sunspot*" *flare.*

A possible location for a "sunspot" type flare is shown hatched on the above figure. The projections of the lines of magnetic force from the dividing plane on to the Sun's surface are shown by broken lines.

In contrast with flares which lie on current paths passing through a neutral point, flares on paths passing into sunspots should in general extend outwards

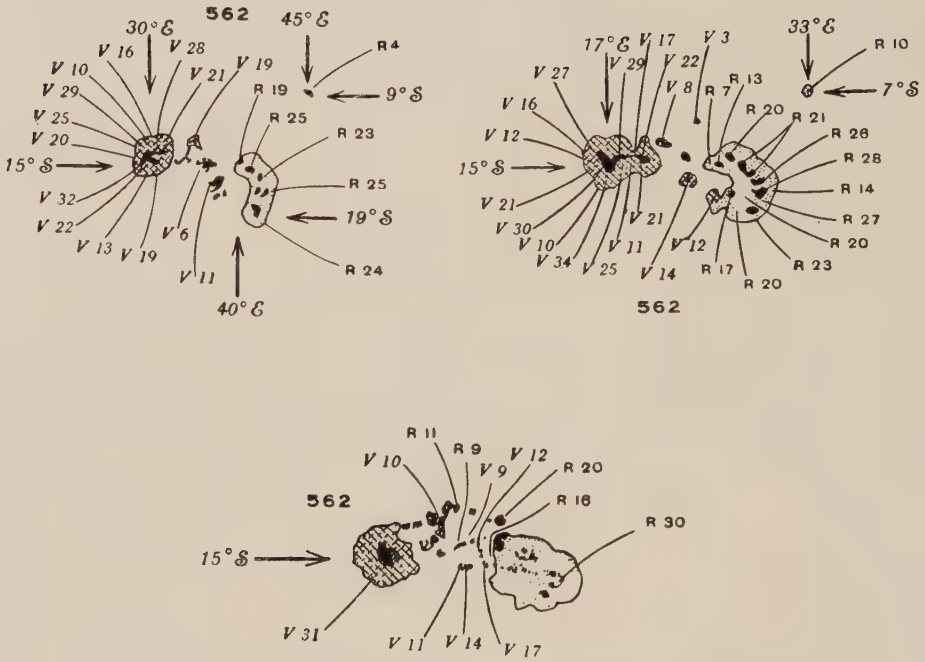

FIG. 5.—*The great spot group of 1917 February 7.*

The above drawings, made at Mount Wilson, show in order the appearances of spot group Mt. Wilson No. 562, at intervals of 24 hours, on 1917 February 6, 7 and 8. The polarities are indicated by the letters V or R, and the field strengths are given in units of 100 gauss. Note the development, in the time between the second and third sketches, of minor spots of random polarities in the region between the two main spots.

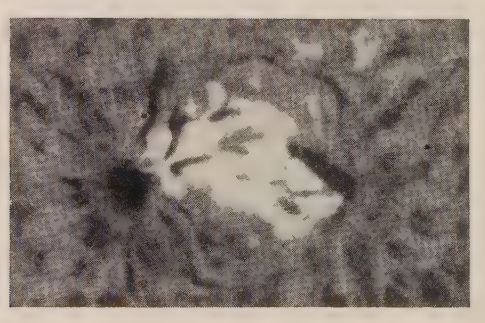

FIG. 6.—*Chromospheric flare of 1917 February 7.*

The flare of 1917 February 7, a few minutes after the second drawing of Fig. 5 was made. The general shape is in good agreement with that suggested in Fig. 4.

from near the sunspot and occupy larger areas. Fig. 3 shows the possible appearance of a flare of the type discussed above.

7. *Flares in Multiple Spot Groups.*—We have so far applied this theory of the origin of flares only to the simple case of an idealized bipolar pair of sunspots. Owing to lack of precise information on the distribution and rate of growth of the magnetic fields and the lack of an accepted mechanism of sunspot growth, it is not desirable to examine in much detail at this stage the possible location of flares in more complicated systems. We shall, however, state briefly the predictions of the theory for the case of a system consisting of two large stable sunspots between which is growing a pair of small sunspots with its line of centres approximately perpendicular to the line joining the two main sunspots. This is a fairly common system. It may be worth noting that in this case the particular mechanism of sunspot growth has hardly any influence on our predictions.

Fig. 4 indicates the lines of magnetic force near the surface for such a case. We suppose all the flux from each of the minor spots to be captured by the major sunspots, although this is not essential to the argument. Then as the minor spots

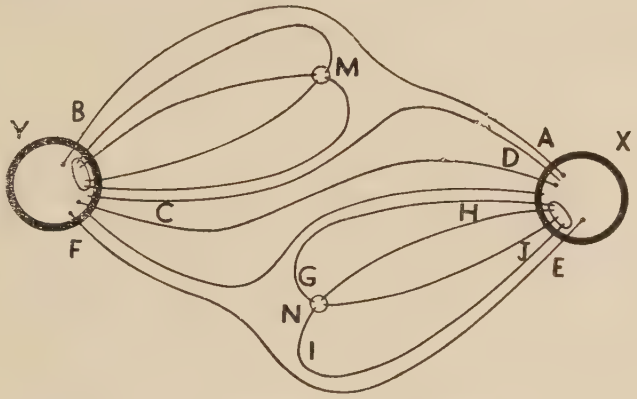

FIG. 4.—*Lines of magnetic force in a complex spot group.*

Lines of magnetic force are shown for a spot group consisting of two fully-developed major spots, X and Y, and two minor spots M and N growing with their line of centres perpendicular to the axis of the group.

grow, currents may flow along paths such as AB, CD, EF, joining the major sunspots. Moreover, currents can also flow along lines of magnetic force joining the minor spots with the major spots; paths such as GH, which cross the line joining the minor spots, will carry more current than paths such as IJ, for the induced e.m.f. is clearly greater along the former than along the latter.

Flares may now appear along parts of lines of force such as AB, CD, EF, GH, particularly where such lines crowd together, thereby increasing the resistance and field strengths. The great flare of 1917 February 7 seems to have originated in this way. Sunspot magnetic fields and polarities on the mornings of the flare and before and after the flare, are shown in Fig. 5 (Plate 3) (**16**), and considerable development of minor sunspots has taken place during this period. Fig. 6 (Plate 3) shows the flare within a few minutes of the second sunspot drawing (**17**). The general shape is in very good agreement with that suggested by Fig. 4.

8. *The Emission of Radiation from Flares.*—We shall now estimate the intensity of the radiation emitted in a flare and compare it with observation. This is done first for a flare on a current path which passes through a neutral point and then for

a flare on a current path passing into a sunspot. The method involves, on the one hand, estimates of the dimensions of a flare and the mean free time between inelastic collisions, from which the number of excitations per second may be computed, and on the other hand, estimates of the total number of excitations based on observed $H\alpha$ intensities.

From our equation for the rate of gain of electron energy in crossed electric and magnetic fields, it has been computed that for H zero and an electric field of $1{\cdot}6 \times 10^5$ e.m.u. (i.e. a little greater than E_c when the electron concentration is 10^{11} per c.c.), and assuming electron energies cannot exceed 10·1 e.V. owing to inelastic collisions with hydrogen atoms, the mean time τ between inelastic collisions will be $2{\cdot}8 \times 10^{-3}$ sec. (**9**). The time required to reach a given energy for the appropriate critical field at different electron (or positive ion) concentrations is inversely proportional to the electron concentration. Thus for a field just exceeding the critical field, τ will be approximately $2{\cdot}8 \times 10^8/n$ sec., or $2{\cdot}2 \times 10^{-4}/p$ sec.

H is zero only at the neutral point. Elsewhere across a flare near the neutral point H is finite, but it still has little influence on the rate of energy gain in a given electric field unless

$$e^2H^2u^6/\pi^2\beta^4N_+^2m^2Z^4 > 1,$$

i.e.

$$Hu^3/N_+ > 2{\cdot}5 \times 10^{11}.$$

For u equal to $1{\cdot}89 \times 10^8$ cm./sec. (corresponding to 10·1 e.V. electrons) H must exceed $3{\cdot}7 \times 10^{-14}N_+$ before the effect of the magnetic field need be considered.

If Hu^3 be great enough, then the rate of gain of energy simplifies to

$$\frac{dW}{dt} = \frac{E^2\pi\beta^2N_+mZ^2}{H^2u^3} - \frac{\pi\beta^2m^2N_+Z^2}{Mu}\left(1 - \frac{u_0^2}{u^2}\right),$$

and becomes zero when

$$E^2/H^2 = (m/M) \,.\, (u^2 - u_0^2).$$

Thus, due to the electric field, the increase in the average electron energy is $ME^2/2H^2$. For it to exceed 10.1 e.V., E/H must be greater than $4{\cdot}4 \times 10^6$ e.m.u. Putting, arbitrarily, $E = E_c$, H must be less than $3 \times 10^{-13}N_+$, or $0{\cdot}5p$, a value of H for which the above simplification is justifiable. It may be noted that the conductivity is not seriously affected until $H > 2p$.

In the dividing plane near the neutral point $H = 2G \sin\theta/2$, θ being the angle between the radius vector from the associated sunspot and the line joining the sunspot and neutral point. H has a value $0{\cdot}5p$ at a distance $3{\cdot}5 \times 10^7p$ cm. from the neutral point; as p is in general less than 0·1 dyne/cm.^{2}, the region over which $H < 0{\cdot}5p$ has a circular section of diameter 70 km. or less. This is a rather arbitrary lower limit to the width of a flare. If E exceeds E_c, for example, the width will be proportionately greater; but in the dividing plane we may well expect E to increase away from the neutral point as the conductivity decreases. The effect of currents perpendicular to the magnetic field is difficult to discuss quantitatively, but undoubtedly increases the above calculated width of the flare.

The observed width of flares, say 2000 km., may well be larger than the real width, as even under good atmospheric conditions the resolution of a spectrohelioscope is limited to about 1000 km. Moreover, as flares are known to be optically thick, it is to be expected that a narrow excited region will be greatly broadened by absorption and re-emission of $H\alpha$ radiation.

It will be assumed, for simplicity, that across the predicted flare the rate of excitation equals that at the centre of the section. Then in a section of unit width parallel to the dividing plane, the total number of excitations per second, when E just exceeds the appropriate E_c, is $2{\cdot}3 \times 10^{31} p^4$. The flare will generally be observed at an angle to the dividing plane, and the total number of excitations in a section 1 cm. wide cut by planes containing the line of sight will be greater than this, but still of the same order.

In arriving at this estimate we have assumed inelastic collisions to occur as soon as the excitation potential is reached. In reality this will not occur. Electrons have energies greater than thermal after inelastic collisions, and the mean time between collisions is thus reduced. Neither have we discussed the effect of changes in the medium following the onset of a flare, such as increases in electron pressure and concentration.

It is of importance to discuss the effects when the electric field considerably exceeds E_c. Such a field seems quite possible, and may give rise to an appreciable increase in the excitation rate. To see what is involved here, suppose $E = E_L$. Then $\tau = \lambda/u = 1{\cdot}4 \times 10^7/N$ sec. and the number of excitations per sec. in a 1 cm. section near the neutral point is $3{\cdot}6 \times 10^{20} p^3 N$. According to the data in Table I the number of excitations per sec. increases under these conditions by a factor of about 10^3 at the bottom of the chromosphere and by a smaller factor at greater heights.

As a result of these effects, the above computations can be regarded as giving only the order of magnitude of the number of excitations per second.

The actual amount of radiation emitted may be estimated from flare observations as follows. The observed $H\alpha$ emission line in an average flare has an intensity about three-quarters of that of the neighbouring continuous spectrum, while its effective width $\Delta\lambda$ may be taken to be approximately 1 A. Flares themselves are frequently observed in the forms of filaments of width about 2000 km. For a unit section the surface area S over which the emission takes place across the flare is approximately πD, where D is the observed flare width, i. e. 2000 km., it being assumed that emission from the faces of this section is balanced by radiation received from the adjacent sections. Moreover, since I_λ is three-quarters of the black-body emission at 5750 deg. K., the energy emitted in $H\alpha$ is

$$\int\int I_\lambda \, . \, d\lambda \, . \, dS = 3\pi^2 hc^2 D \, . \, \Delta\lambda / 2\lambda^5 \{\exp(c_2/\lambda T) - 1\},$$

and the number of quanta emitted is

$$3\pi^2 cD \, . \, \Delta\lambda / 2\lambda^4 \{\exp(c_2/\lambda T) - 1\},$$

or $1{\cdot}1 \times 10^{27}$ per sec.

With an observed number of $H\alpha$ quanta and a mechanism for producing the radiation, it is now possible to estimate the total number of excitations per second. Unfortunately, information is scanty on the cross-sections of hydrogen atoms for excitation to various energy levels subsequent to collision with electrons of the energies considered. No experimental results are available for these cross-sections, while no satisfactory theoretical analysis has been made. Bethe (**14**), however, has madea detailed examination of the relative cross-sections for various types of collision of high velocity electrons with hydrogen atoms, and from his results it appears that the relative probabilities of excitation to the 2-quantum and 3-quantum levels, for electrons of energy 1000 volts, are in the ratio 6·8 : 1. For

the present discussion it is assumed that the corresponding excitation cross-sections for electrons of energies slightly greater than the excitation potentials are in the ratio 7 : 1.

Now consider what happens after an excitation to the 3-quantum level. The ratio of the probabilities of a $3 \rightarrow 2$ and a $3 \rightarrow 1$ transition is 1 : 1·27 (**15**). If an electron makes a $3 \rightarrow 1$ transition, the quantum emitted, being resonance radiation, has a much higher chance of being reabsorbed rapidly than a quantum emitted from a $3 \rightarrow 2$ transition. The process of absorption and emission continues until a $3 \rightarrow 2$ transition occurs. It is clear that the final result of an excitation to the 3-quantum state is almost certainly the emission of an $H\alpha$ quantum and an $L\alpha$ quantum, the relative intensity of $L\beta$ being weak. It also follows that excitations to higher levels will give rise to a member of the Balmer series and an $L\alpha$ quantum. But it is well known that the $H\alpha$ line is by far the most important of the Balmer lines in flares, and the other lines may be neglected in comparison with it. Thus to a first approximation every excitation to a level higher than the 2-quantum state gives rise to one $H\alpha$ and one $L\alpha$ quantum. The number of $L\alpha$ quanta emitted cannot be less than the number of $H\alpha$ quanta, and it cannot well exceed the number of $H\alpha$ quanta by a factor of more than about 7 unless a large fraction of electrons make inelastic collisions after acquiring enough energy to excite the 2- and not the 3-quantum level. As an estimate, then, we shall take the number of $L\alpha$ quanta emitted, and also the total number of excitations, to be about seven times the number of $H\alpha$ quanta.

On the above basis, the number of excitations in a 1 cm. wide section through a typical flare, estimated from observations, is about $7{\cdot}7 \times 10^{27}$ per second as compared with the predicted number of $2{\cdot}3 \times 10^{31} p^4$. Since p may be as large as 0·1 dyne/cm.^{2}, the agreement between the above results is satisfactory in view of the wide range of variation to be expected between different flares, and the considerable uncertainty involved in the estimates made.

It is a simple matter to extend the above treatment to a flare which occurs on a current path which passes into a sunspot. Suppose the thickness of a flare in the line of sight to be l. Then the number of excitations per second in a column of length l and unit cross-section is $\int (n/\tau) dl$. For a field just greater than E_c, this is $n^2 l / 2{\cdot}8 \times 10^8$ if n be constant throughout. If the emission of radiation be only from the two ends of this column, then the observed intensity of radiation corresponds to $3{\cdot}5 \times 10^{17}$ excitations per second within the column. Equating the predicted and observed excitation rates,

$$n^2 l = 10^{26} \text{ cm.}^{-5}.$$

If $n = 10^{10}$, this calculation gives a column about 10 km. thick, and the flare is presumably confined to the neighbourhood of the dividing plane. We may infer from this result that even if E is rather less than E_c, excitations may take place throughout a larger volume at a sufficient rate for a flare to occur.

9. *Discussion.*—We have shown how the distribution of positive ions and neutral atoms in the chromosphere and the magnitude of the induced electric field near sunspots in general confine flares to the chromosphere, as is well known from observation; but should the necessary concentrations and field be present, flares would also be predicted in prominences, and it is of significance that such flares have occasionally been observed.

The present theory has been applied to an ideal bipolar pair of growing sunspots, and to one case of the more complex groups. Although these applications have been limited, the correlations of observed phenomena with sunspots of various type seem to be those which we would generally expect on the basis of this theory.

Basic information on the concentrations and temperatures of electrons and neutral atoms at various heights seems at present too inaccurate to warrant a more detailed treatment than has been given. Lack of knowledge of the internal electrical resistance and the manner of creation of sunspots has rendered uncertain the predictions of the locations of flares. We have assumed sunspots to be formed when a sub-surface magnetic toroid reaches the surface, in which case some type of disturbance might be expected along the line joining two growing sunspots, whereas none is observed. While the exact manner of sunspot growth is not of importance to the validity of the present theory, it materially affects details of the expected location and form of flares. Observations of these may throw light on theories of sunspots.

Mathematical difficulties have enforced simplifications in treating the excitation resulting from an electric field, and this would be worth more detailed analysis. Moreover, approximations made to the electrical conductivity in the presence of a magnetic field may have introduced appreciable errors in the predicted electric field strengths near the neutral point.

Acknowledgments

The author wishes to thank many officers of the Division of Physics, Council for Scientific and Industrial Research, in particular Dr G. H. Briggs and Mr J. Mackenzie, for many valuable discussions; and also Dr C. W. Allen and Dr D. F. Martyn of the Commonwealth Observatory, who gave helpful criticism in the early development of the above theory; thanks are also due to the Editors of the University of Chicago Press for permission to reproduce Fig. 6 (Plate 3) from the *Astrophysical Journal*, **73**, 1931.

The above investigation has been carried out as part of the programme of the Commonwealth Council for Scientific and Industrial Research.

Commonwealth Council for Scientific and Industrial Research,
Division of Physics, National Standards Laboratory,
Chippendale, Sydney :
1948 *February* 27.

References

(1) Allen, C. W., *M.N.*, **100**, 635, 1940.
(2) Waldmeier, M., *Z. Astrophys.*, **16**, 276, 1938.
(3) Ellison, M. A., *M.N.*, **103**, 3, 1943.
(4) Giovanelli, R. G., *Ap. J.*, **91**, 334, 1940.
(5) Giovanelli, R. G., *Ap. J.*, **89**, 555, 1939.
(6) Waldmeier, M., *Z. Astrophys.*, **20**, 46, 1940.
(7) Giovanelli, R. G. and Higgs, A. J., *Terr. Mag. atmos. Elect.*, **44**, 181, 1939.
(8) Giovanelli, R. G., *Nature*, **158**, 81, 1946.
(9) Giovanelli, R. G., *Phil. Mag.*, " Electron Energies Resulting from an Electric Field in a Highly Ionized Gas ". (In the press).
(10) Cowling, T. G., *Proc. Roy. Soc.*, **183**, 453, 1945.
(11) Cillié, G. G. and Menzel, D. H., *Harvard College Observatory Circular* 410, 1935.

(12) Giovanelli, R. G., *M.N.*, **107**, 338, 1947.
(13) Alfvén, H., *M.N.*, **105**, 3, 1945.
(14) Bethe, H., *Handbuch der Physik*, 519 (2nd Edition, XXIV/I, 1933).
(15) Menzel, D. H. and Pekeris, C. L., *M.N.*, **96**, 77, 1935.
(16) Hale, G. E. and Nicholson, S. B., " *Magnetic Observations of Sunspots*, 1917–1924 ", Carnegie Institution of Washington, 1938.
(17) Hale, G. E., *Ap. J.*, **73**, 379, 1931.

MEAN AREAS AND HELIOGRAPHIC LATITUDES OF SUNSPOTS IN THE YEAR 1940

Royal Observatory, Greenwich

(Communicated by the Astronomer Royal)
(Received 1948 March 1)

The following results are in continuation of those given in *M.N.*, **107,** 468, 1947, and are derived from the measurement at Greenwich of photographs taken at the Royal Observatories of Greenwich and the Cape and at the Kodaikanal Observatory, India. For one day, November 16, a plate for measurement was kindly supplied by the Superintendent, U.S. Naval Observatory, Washington.

Table I gives the mean daily areas of umbrae, whole spots and faculae for each synodic rotation of the Sun included in the year 1940; the means for the year as a whole are included in Table II, which summarizes the yearly values from 1933–40.

Table III gives for each rotation in the year 1940 the mean daily area of the whole spots (corrected for foreshortening) and the mean heliographic latitude of the spotted areas for both northern and southern hemispheres.

The mean heliographic latitude of the entire spotted area and the mean distance from the equator of all spots are also tabulated. The mean values for the year 1940 are included in Table IV.

Tables II and IV are in continuation of similar tables given in *Monthly Notices* : for the years 1874 to 1888—**49,** 381–382; 1889 to 1902—**63,** 465–466; 1901 to 1914—**76,** 402–403; 1913 to 1924—**85,** 1007–1008; 1923 to 1933—**94,** 870–871.

The rotations in Tables I and III are numbered in continuation of Carrington's series.

The chief features of this record for the year 1940 are as follows :—

(1) The decline from solar maximum conditions, noted in 1939, was unmistakable in 1940. The mean daily spotted area of 1039 millionths of the Sun's hemisphere was half that of the maximum years 1937–38. Nevertheless, the year 1940 was an active one, and on no day were spots absent.

From rotation to rotation, sunspot and facula mean areas were more evenly maintained than in 1939. Mean daily areas for spots ranged from 553 millionths in rotation 1158 to 1683 in rotation 1162 (Table I, Col. 8). For faculae, the areas ranged from 1079 millionths in rotation 1159 to 1831 in rotation 1163.

(2) As in each preceding year (except 1937) of the present cycle, the southern hemisphere had the greater spotted area.

(3) The number of spot groups lasting for two days or longer was 282 as compared with 371 in the preceding year. Of these, 125 were in the northern hemisphere and 157 in the southern. In addition, there were 84 spots, mostly very small, seen on one day only; 41 were in the northern hemisphere and 43 in the southern.

There were 17 spot groups with an average area during their disk transits greater than 500 millionths (corrected for foreshortening) of the Sun's hemisphere —i. e. they were all possible naked-eye spots when not strongly foreshortened towards the Sun's limb. The largest of these was Group 13502 with central meridian passage on January 5 and an average area of 1689 millionths. This

TABLE I

No. of Rotation	Rotation Commenced U.T.	Days Photo-graphed	Mean Daily Areas					
			Projected *			Corrected for Foreshortening †		
			Umbrae	Whole Spots	Faculae	Umbrae	Whole Spots	Faculae
1154	1939 Dec. 18·30	28	289	1432	1392	199	998	1686
1155	1940 Jan. 14·63	27	259	1383	1436	186	1021	1762
1156	Feb. 10·97	27	272	1429	1207	201	1081	1513
1157	Mar. 9·31	28	340	1814	1073	242	1309	1357
1158	Apr. 5·61	27	155	752	1194	115	553	1501
1159	May 2·86	27	200	994	843	144	711	1079
1160	May 30·08	27	319	1553	1160	228	1125	1419
1161	June 26·28	27	287	1534	1243	215	1152	1522
1162	July 23·48	28	469	2433	1212	326	1683	1515
1163	Aug. 19·71	27	315	1499	1466	226	1082	1831
1164	Sept. 15·96	27	277	1443	1339	211	1126	1702
1165	Oct. 13·24	28	221	1150	1136	157	817	1393
1166	Nov. 9·54	27	180	953	1314	127	685	1553
1167	Dec. 6·86	27	225	1214	1200	158	864	1531

* Expressed in millionths of the Sun's disk.
† Expressed in millionths of the Sun's hemisphere.

TABLE II

Year	No. of Days		Mean Daily Areas					
			Projected*			Corrected for Foreshortening†		
	Photographed	Without Spots	Umbrae	Whole Spots	Faculae	Umbrae	Whole Spots	Faculae
1933	365	234	24	120	225	18	88	267
1934	365	145	27	142	227	22	119	354
1935	365	21	152	810	910	117	624	1100
1936	366	0	288	1529	2106	217	1141	2545
1937	365	0	509	2795	2856	375	2074	3505
1938	365	0	501	2706	2578	371	2019	3205
1939	365	0	404	2163	1907	295	1579	2349
1940	366	0	279	1434	1224	200	1039	1522

* Expressed in millionths of the Sun's disk.
† Expressed in millionths of the Sun's hemisphere.

TABLE III

No. of Rotation	Rotation Commenced U.T.	Spots North of the Equator		Spots South of the Equator		Mean Latitude of Entire Spotted Area	Mean Distance from Equator of all Spots
		Mean Daily Area	Mean Heliographic Latitude	Mean Daily Area	Mean Heliographic Latitude		
			°		°	°	°
1154	1939 Dec. 18·30	808	12·50	190	11·33	+7·97	12·28
1155	1940 Jan. 14·63	617	10·88	405	11·48	+2·02	11·11
1156	Feb. 10·97	337	9·93	744	9·09	−3·17	9·35
1157	Mar. 9·31	916	12·55	393	9·46	+5·94	11·62
1158	Apr. 5·61	231	10·40	322	9·29	−1·06	9·75
1159	May 2·86	345	13·59	366	8·82	+2·06	11·14
1160	May 30·08	188	13·59	937	13·13	−8·67	13·21
1161	June 26·28	685	11·68	467	14·18	+1·20	12·70
1162	July 23·48	770	11·15	913	12·28	−1·53	11·73
1163	Aug. 19·71	404	11·49	678	8·84	−1·26	9·83
1164	Sept. 15·96	451	14·51	675	7·93	+1·05	10·56
1165	Oct. 13·24	193	13·32	624	11·00	−5·25	11·55
1166	Nov. 9·54	442	11·68	243	11·96	+3·30	11·77
1167	Dec. 6·86	424	9·18	441	10·79	−1·01	10·00

TABLE IV

Year	Days Photographed	Spots North of the Equator: Mean Daily Area	Spots North of the Equator: Mean Heliographic Latitude	Spots South of the Equator: Mean Daily Area	Spots South of the Equator: Mean Heliographic Latitude	Mean Latitude of Entire Spotted Area	Mean Distance from Equator of all Spots
			°		°	°	°
1933	365	86	10·60	2	8·35	+10·23	10·56
1934	365	44	16·45	74	28·09	−11·49	23·75
1934	365 (Old Cycle)	19	4·10	1	4·37	+ 3·79	4·11
	365 (New Cycle)	26	25·44	74	28·31	−14·46	27·57
1935	365	205	22·42	419	23·72	− 8·57	23·30
1936	366	463	19·36	678	21·02	− 4·63	20·35
1937	365	1317	17·63	757	15·96	+ 5·36	17·02
1938	365	899	15·55	1120	14·17	− 0·94	14·79
1939	365	649	14·64	931	12·57	− 1·39	13·42
1940	366	499	11·65	540	10·72	+ 0·03	11·17

largest group with its return and six others from the list of 17 big spots all fell within the limited longitude range of 45°, viz. 92°–136°.

(4) The equator-ward progression of the spot zones was continued from the opening years of the cycle, the mean weighted latitude of 11°·17 being 2°·3 lower than in 1939. Latitudes of individual spots lasting for two days or longer ranged from 1° to 28°; a one-day spot was recorded in north latitude 32°. The centre of gravity of the latitudes of all spots, weighted according to areas, was on the Sun's equator (Table IV, Col. 7).

Royal Observatory,
Greenwich :
1948 *February* 23.

OBSERVATIONS OF THE SATELLITES OF URANUS

W. H. Steavenson

(Received 1948 May 7)

Summary

1. Observations of the position-angles of Umbriel, Titania and Oberon show that the errors, if any, in the assumed periods of these satellites are small.

2. Observations of the position-angle of Ariel indicate a correction to the computed longitude of about $+6°{\cdot}1$, corresponding to a shortening of the accepted period by $0^{s}{\cdot}34$.

3. New values are suggested for the stellar magnitudes of the satellites, which are brighter than previously estimated.

4. There is variability in the light of one or both of the two outer satellites, pointing to a considerable inclination of their axes of rotation to the normals to the orbit-planes.

Observations of position-angle.—Observations of the apparent position-angles of the four chief satellites of Uranus were made with the 30-inch reflector on several nights between 1947 January 9 and 1948 April 8. As the orbits were seen in projection almost as circles it was possible to assume uniformity of apparent angular motion, so that observations of position-angle could be used to give a direct check on the computed longitudes of the satellites at any point, at least within the probable error of the measures. The ephemerides computed at the United States Naval Observatory and published annually in the *Nautical Almanac* and elsewhere are not intended for the rigorous comparison of observation with theory, but they serve the purpose of an approximate check and are accurate within a few tenths of a degree.

A few observations of Oberon, Titania and Umbriel sufficed to show that either there were no sensible errors in the computed longitudes or that such errors were so small that their exact amounts could only be determined by means of a very great number of observations. The results of the measures are given below.

Oberon

Date	U.T.	Obsd. P.A.	Compd. P.A.	O–C	Number of settings
	d h m	°	°	°	
1947 Jan. 9	22 33	175·8	176·4	−0·6	10
1948 Mar. 27	20 41	215·6	216·0	−0·4	15

Titania

1947 Jan. 9	22 10	24·1	23·6	+0·5	10
1948 Mar. 24	19 45	195·0	195·8	−0·8	10

Umbriel

1947 Jan. 13	22 48	255·8	256·6	−0·8	5
22	18 28	210·1	210·1	0·0	4
1948 Mar. 22	20 26	6·0	5·3	+0·7	12

In the case of Ariel the discrepancy between theory and observation was so large in comparison with the probable error of the measures that it was obviously real and seemed to justify an attempt to obtain an approximate value for the error in the longitude by means of a more extended series of observations. At the same time it became necessary, in order to secure a fair comparison, that the longitudes should be rigorously computed from the elements of the orbit derived by Newcomb and used ever since in the computation of the Nautical Almanac ephemeris.

At my request Dr J. G. Porter very kindly undertook this labour and I wish here to make warm acknowledgment of my indebtedness to him, and to Mr J. A. Bancroft-Wilson, who carried out a check of Dr Porter's figures. The results of the measures were as follows:

Ariel

Date		U.T.	Obsd. P.A.	Compd. P.A.	O–C	Number of settings
	d	h m	°	°	°	
1947 Jan.	9	21 49	347·5	358·8	−11·3	6
	13	21 32	139·3	148·9	− 9·6	12
	17	20 56	295·5	301·2	− 5·7	15
	22	17 54	310·9	325·0	−14·1	10
	23	20 50	161·8	164·8	− 3·0	12
	26	22 00	83·6	89·6	− 6·0	6
Mar.	24	21 14	227·9	233·5	− 5·6	6
Nov.	23	21 54	293·6	299·2	− 5·6	10
Dec.	29	20 50	198·4	202·4	− 4·0	6
	30	20 48	53·0	60·3	− 7·3	10
1948 Jan.	14	20 51	73·0	77·5	− 4·5	20
	19	20 39	79·0	84·4	− 5·4	25
	31	20 13	166·5	172·1	− 5·6	4
Feb.	2	21 18	232·3	240·8	− 8·5	20
	3	20 47	96·0	100·9	− 4·9	20
	9	20 23	316·7	325·7	− 9·0	10
	10	20 48	174·5	180·4	− 5·9	20
Mar.	1	20 45	196·6	204·5	− 7·9	23
	20	20 20	11·1	13·2	− 2·1	20
	25	20 11	17·1	20·1	− 3·0	15
	30	20 21	23·8	25·2	− 1·4	10
Apr.	6	20 10	102·3	106·9	− 4·6	10
	8	20 27	172·9	179·0	− 6·1	14

It will be seen from the above figures that all values of O–C are negative and that the average error in the longitude at the epoch 1947.80 amounts to 6°·1 or 61·5 minutes of time. As the motion of the satellites at the present time is clockwise, this corresponds to an error in the longitude of positive sign, Ariel being ahead of its computed position by the amount stated. Since the epoch of Newcomb's orbit is 1872.0, this corresponds to a shortening of the computed period by about $0^{s}\cdot34$. This is a very small error when considered in relation to the shortness of the time elapsed between the discovery of the satellite, in 1847, and Newcomb's computation of its orbit. The period now becomes $2^{d}\cdot5203796$ instead of $2^{d}\cdot5203830$.

An inter-comparison of the figures in the O–C column above might suggest that the observations were subject to very considerable errors, amounting in some cases to several degrees. The measures involved were certainly delicate,

but on any one night the settings agreed very well among themselves, showing a probable accidental error of about 0°·2 or less. With a view to investigating the possibility of some irregular errors inherent in the method employed, a double star of similar separation (15″ ±) and a difference of six magnitudes in the components was measured on eight nights, ten to fifteen settings being made on each occasion. The extreme difference between any two nights was 1°·3, and the results on six of the nights lay within 0°·3 of a mean value. I am therefore led to believe that the large differences shown between some of the figures in the O–C column are at least partly real, but am unable to suggest an explanation of them.

Brightness of the Satellites.—The values generally adopted for the stellar magnitudes of the satellites are *, for Oberon 14^m, for Titania 14^m, for Umbriel 16^m–17^m, and for Ariel 16^m. Actually the satellites are a good deal brighter, and this is particularly the case with the two inner ones, where too little allowance has been made for the swamping effect of the light of the planet. I have made no actual photometric measures, but from familiarity with the North Polar Sequence and the fields of numerous variable stars I am confident that the following figures are closer to the truth than those quoted above:

	m
Oberon	13·8
Titania	13·7
Umbriel	14·5
Ariel	13·7

The two inner satellites can only be clearly seen with the 30-inch telescope when the planet is hidden behind a field-bar. Ariel is then easier to see and measure than the more distant Umbriel and certainly is closely comparable in brightness with Titania, though of course far more difficult to see and measure. The field-bar employed consisted of a thin sheet of dark red transparent gelatine, covering half the field and bounded by a carefully cut straight edge. Position-angles were measured by setting this edge at right angles to the line joining planet and satellite, the former being behind the bar but still clearly visible. The results obtained by this method are surprisingly consistent and seem to be comparable in accuracy with measures made in the ordinary way by alignment with a wire.

I made careful comparisons of the brightness of Titania and Oberon on 26 nights between 1946 December 28 and 1948 April 8 and was surprised to find very definite differences from night to night. Such differences, which can only be due to rotation, were often observed by me some 20 years ago, when the Earth was not far from the plane of the orbits, but were hardly to be expected now that the line of sight is nearly at right angles to that plane. The variations seem to indicate that the axis of rotation of one or both of the satellites makes a very considerable angle with the normal to the orbit-plane, and it may possibly lie in or close to that plane. I am not able to say whether the changes observed affect both or only one of the satellites. Generally Titania was definitely the brighter of the two, sometimes by as much as $0^m·3$, and on two occasions only it was between $0^m·1$ and $0^m·2$ fainter than the other. The mean of all the observations makes Titania the brighter by $0^m·12$.

Cambridge:
1948 *May* 6.

* Newcomb and Vogel, quoted in *B.A.A. Handbook* 1948, p. 61.

OBSERVATIONS OF NOVAE, 1947.

W. H. Steavenson

(Received 1948 May 7)

The observations here recorded were all made with the 30-inch Hindle reflector and are in continuation of the series communicated to the Society in past years.

Nova Aquilae (1918)

Observed on five nights. This nova is perhaps still slightly variable, as it is reported to have been before its outburst; so the individual estimates are given.

Date	Mag.
1947 June 15	11·3
22	11·3
July 7	11·2
Aug. 26	11·2
Sept. 12	11·6

There is nothing peculiar about the colour or character of the image, which appears white and purely stellar.

Nova Aquilae No. 6 (1936)

The general fading of this nova appears now to have ceased and there is no certain evidence of variability.

Date	Mag.
1947 June 12	15·7
July 22	15·7
Aug. 9	15·7
Sept. 10	15·8
Oct. 14	15·8

Nova Aquilae (1945)

Fading continues fairly steadily, the nova dropping about a magnitude in the period covered by the observations. There is nothing peculiar about the appearance of its image.

Date	Mag.	Date	Mag.	Date	Mag.
1947 May 16	14·2	1947 Aug. 3	14·4	1947 Sept. 1	14·6
June 12	14·4	6	14·5	8	14·6
15	14·4	9	14·5	10	14·7
17	14·6	16	14·6	12	14·7
19	14·6	19	14·7	16	14·7
July 5	14·4	22	14·5	21	14·7
22	14·5	24	14·6	23	14·8
26	14·4	26	14·6	Oct. 3	14·8
27	14·4	27	14·7	14	15·1

Nova (*T*) *Coronae* (1866)

Observed on one night, May 16, when the magnitude was estimated to be 9·56. The colour was pale yellow, as it was before the outburst of 1946 February. The nova had faded to about its previous level of brightness by 1946 May and the estimate given above makes it a quarter of a magnitude brighter than it was then.

Nova Cygni (1876)

This is one of the novae that are slightly but definitely variable. I therefore give all the individual estimates of brightness.

Date	Mag.	Date	Mag.	Date	Mag.
1947 June 12	15·00	1947 Aug. 9	14·76	1947 Sept. 2	14·81
15	15·10	16	14·81	10	14·81
17	15·10	19	14·76	12	14·86
19	15·05	24	14·76	21	14·81
July 5	15·00	25	14·81	23	14·71
22	15·00	26	14·86	Oct. 3	14·65
26	14·86	27	14·76	4	14·76
27	14·91	28	14·71	12	14·76
Aug. 3	15·00	31	14·76	14	14·71
6	14·81	Sept. 1	14·81		

Nova Cygni (1920)

Observed on May 16, June 15 and August 9 and estimated on all three occasions to be of magnitude 15·7. There has been no sensible change in the light of this nova for many years past.

Nova Cygni (1942)

This nova is still fading very slowly and was definitely a few tenths of a magnitude fainter in 1947 than in 1946.

Date	Mag.	Date	Mag.
1947 June 12	15·7	1947 Aug. 22	15·8
15	15·7	24	15·8
July 5	16·0	Sept. 10	15·8
22	15·9	23	15·9
Aug. 9	15·9		

Nova Herculis (1934)

There has been no sensible change in the light of this nova during the past three years. In 1947 it was observed on eleven nights between April 12 and August 31 and estimated to be of magnitude 13·2 or 13·3 on each occasion. Under a high power it still appears as a small round planetary nebula, about 3 sec. of arc in diameter, of a greenish colour and having an apparently stellar nucleus.

Nova Lacertae (1910)

Sensibly constant in light. Estimated magnitude on June 17 was 14·2, and on September 12, 14·4.

Nova Lacertae (1936)

This nova has ceased to fade and is steady in its light. Observed on June 15, August 19 and September 12 and estimated at $14^{m}\cdot8$ on each occasion.

Nova Lyrae (1919)

The light of this nova has been steady for many years. Observed on June 12, 15, 19 and August 9, and estimated at $15^{m}\cdot3$ on each of these nights.

Nova Ophiuchi (1848)

This is another of the slightly variable novae.

Date	Mag.	Date	Mag.
1947 May 16	12·7	1947 Aug. 3	12·7
June 12	12·7	6	12·5
15	12·5	9	12·5
17	12·6	19	12·3
19	12·5	26	12·6
July 5	12·4	Sept. 2	12·7
22	12·6	10	12·6
26	12·7		

Nova Persei (1901)

The most markedly variable of all the old novae. The range was less in 1947 than in some other years, amounting to about $0^{m}\cdot9$. The nebulosity that was formerly observable closely south-preceding the nova is no longer perceptible to my eye with the 30-inch telescope, though it was an easy object a few years ago with a much smaller instrument.

Date	Mag.	Date	Mag.	Date	Mag.
1947 June 19	12·95	1947 Aug. 27	13·31	1947 Oct. 5	12·95
July 5	13·05	28	13·20	11	12·79
22	12·84	31	13·26	12	12·95
27	13·00	Sept. 1	13·05	14	12·53
Aug. 3	13·41	8	13·10	25	12·64
6	13·00	10	13·05	Nov. 12	13·10
9	13·00	13	13·00	13	12·95
16	12·90	15	13·05	15	12·59
19	12·95	16	13·00	23	12·64
22	13·00	21	12·95	25	12·74
24	13·05	23	13·00	Dec. 29	12·64
25	13·26	Oct. 3	13·36		
26	13·29	4	13·05		

Nova Sagittae (1913)

This nova has returned to its tranquil minimum after the secondary outburst of 1946. Observed on June 17, July 22, August 19 and September 21, the magnitude being estimated at $14^{m}\cdot3$ on each occasion.

Cambridge :
1948 *May* 6.

THE MEASUREMENT OF RADIAL VELOCITY FROM SLITLESS SPECTRA

P. J. Treanor, S.J. *

(Communicated by the Director, University Observatory, Oxford)

(Received 1948 March 5)

Summary

Radial velocity determinations from slitless spectra of faint stars are statistically useful, provided that the accidental errors do not exceed 8 km./sec. and that systematic errors are absent. The " length of spectrum ", " reversion " and " absorption cell " methods of measurement are examined with reference to these requirements. Expressions are derived which relate the accidental errors of each method to the errors of slit spectra, for which empirical values have been obtained from an analysis of the Lick Catalogue. The accidental errors of the slitless methods predicted in this way are compatible with those found in the available observations, and are subsequently used to compare the methods, and to define the conditions in which each may be usefully employed.

Estimates of the effects liable to be produced by temperature change, flexure and field distortion show that these factors are sufficient to produce considerable systematic errors. Such systematic errors are, indeed, found to be present in all observations. These errors can and must be eliminated, by employing a method of reduction which requires only one exposure, and by the use of slitless spectrographs in place of objective prisms.

The failure of early attempts to use the " stellar image " method is accounted for in the light of the preceding discussion. This method is now reinstated in a new form, in which a star image is superimposed upon a spectrum produced by means of a direct-vision prism of special design. The new method should compare favourably with existing methods, and may be profitably combined with them.

As Bok and McCuskey† have pointed out, stellar radial velocities with probable accidental errors of ± 7 to ± 8 km./sec. are sufficiently accurate for the statistical investigation of solar motion, galactic rotation and associated problems. Radial velocities with an accuracy of this order were obtained by Schwarzschild‡ from objective prism spectra, but more recent investigations, particularly at Harvard, have shown that probable errors can only with great difficulty be pushed as low as ± 10 km./sec. in the measurement of large numbers of stars. In view of the rapidity of the slitless methods, and the faintness of the stars that can be reached, it is highly desirable that the various methods of measuring radial velocities from slitless spectra should be further investigated, and it is the purpose of this article first to discuss the origin of the accidental and systematic errors in the existing methods and finally to discuss a modification of an earlier proposal which gives some promise of yielding accurate results.

Part I. Accidental Errors of Existing Methods

1.1. *The Accidental Errors of Slit Spectra.*—The knowledge of the velocity errors of modern temperature-controlled slit-spectrographs is a necessary

* Skynner Student in Astronomy, Balliol College, Oxford.

† B. J. Bok and S. W. McCuskey, *H.C.O. Annals*, **105**, 327, 1937.

‡ K. Schwarzschild, *Pub. Potsdam Obs.*, **69**, 6, 1913.

preliminary to the quantitative investigation of the errors actually associated with slitless spectrography, and of the relative merits of the different methods.

An empirical estimate of slit-spectrograph errors, in their dependence on dispersion and spectral type, has been obtained by means of an analysis of the errors of measurement tabled in the Lick Catalogue of Radial Velocities.* This catalogue lists for each velocity quoted by a particular observatory the probable error r km./sec., the number of observations n on which the measure rests, the dispersion employed and the spectral type of the star. To make the analysis, observations were first grouped according to dispersion and spectral type. For each group the quantity $E = \Sigma rn\sqrt{n}/\Sigma n$, that is, the weighted mean of the probable error for a single observation, was calculated. The presence of a fair number of stars whose velocity is believed to be variable presents a difficulty. If these stars are included, the accidental error will clearly be overestimated. On the other hand, if the only evidence of variability is the abnormally large standard deviations of the velocity measures in the Lick Catalogue, the exclusion of all suspected variables may involve the exclusion of large random errors, and thus lead to an underestimation of the probable error of a single determination. This difficulty was met in the following way. Any observation of a star of which the variability was attested by observations other than those under consideration, was excluded from the count. Two counts were then made, the first including all the remaining stars, the second excluding stars whose large errors are attributed in the Catalogue to velocity variation.

Table I gives the results of this analysis. For each spectral type and dispersion range, the first line gives the probable error E, in km./sec., for the first

TABLE I

Probable Errors in Slit Spectra

d	O, B	A	F, G	K	M
7–12	4·04 (717)	2·42 (647)	1·19 (2372)	0·97 (4120)	1·10 (452)
(A./mm.)	2·90 (370)	1·59 (452)	0·95 (2068)	0·76 (3671)	0·78 (381)
18–25	2·78 (589)	2·94 (696)	1·86 (1162)	1·36 (1680)	1·46 (212)
	2·63 (487)	2·54 (631)	1·58 (993)	1·15 (1520)	1·17 (188)
30–40	6·80 (4511)	6·70 (4729)	2·74 (4515)	2·06 (3801)	2·59 (870)
	6·15 (3663)	5·57 (3495)	2·51 (4298)	2·02 (3726)	2·50 (799)
50–60	6·97 (1215)	...	...	...	...
	3·88 (862)	...	...	...	...
65–75	...	...	3·47 (201)	3·48 (145)	4·06 (158)†
	...	...	3·47 (201)	3·48 (145)	3·81 (141)
115	...	...	...	...	4·22 (161)†
	...	...	...	...	4·22 (161)
First count	$E = 0{\cdot}08d + 3{\cdot}48$ (1)		$E = 0{\cdot}042d + 0{\cdot}81$ (2)		
Second count	$E = 0{\cdot}08d + 2{\cdot}39$ (3)		$E = 0{\cdot}046d + 0{\cdot}46$ (4)		

* J. A. Moore, *Lick Obs. Pub.*, **18**, 1932.

† These are supplementary values from A. H. Joy, *Ap. J.*, **105**, 96, 1947. (75 A./mm.)

count, followed by the number of plates on which this mean value rests. Corresponding values for the second count follow in the second line.

When the results of Table I are plotted graphically, a clear distinction emerges between early type stars (O to A), and later type stars (F to M). For the latter type the relation between E and the dispersion d (A./mm.) approximates to the form $E=Ad+B$, A and B being constants for each spectral type. Least square solutions for each sub-group of later type stars, in which each point was given a weight proportional to the number of plates which it represents, were sufficiently similar to justify the formation of a weighted least square solution for types F to M as one group. The large scatter of the results for early type stars renders their interpretation less certain, but a least square solution has been calculated in a similar way. The solutions appear at the foot of Table I (equations (1) to (4)).

1.2. *The Accidental Errors of Slitless Spectra.*—The usual many-lined comparison spectrum cannot be employed in determining the velocities of stars from slitless spectra. The alternatives which have been suggested fall into two types. In the first type, which includes the "length of spectrum" and "reversion" methods, the velocity is calculated from the distance between stellar spectral lines, without recourse to any terrestrial reference lines. In the second type, the displacement of the stellar lines is measured with respect to terrestrial absorption lines. It has been the practice to use for this purpose the absorption spectrum of an aqueous solution of neodymium chloride. The new conditions introduced by these methods will modify the accidental errors to be expected for a given dispersion and spectral type, and the purpose of the following paragraphs is to discuss these methods, with a view to relating their accidental errors to the corresponding errors for slit spectra.

1.21. *The length of spectrum method.*—This method was suggested by Pickering* and first applied to axial stars by J. S. Plaskett† in the modified form proposed by Orbinsky.‡ The principle of the method is as follows. Two lines, of wave-length λ_R, λ_V, at the red and violet ends of the spectrum of a star with a velocity of recession v, will be displaced from their rest positions by amounts $\delta\lambda_R=\lambda_R v/c$, $\delta\lambda_V=\lambda_V v/c$; c being the velocity of light. If the linear dispersion in mm. per angstrom is K_R at λ_R, K_V at λ_V, the displacement of the lines on the plate will be $\delta x_R=K_R\delta\lambda_R$, $\delta x_V=K_V\delta\lambda_V$. The change in length of the spectrum is therefore

$$\delta l=\delta x_R-\delta x_V=(K_R\lambda_R-K_V\lambda_V)v/c. \qquad (5)$$

In a grating with normal dispersion ($K_R=K_V$) the length is increased by recession. With prismatic dispersion, on the other hand, $K_R\lambda_R<K_V\lambda_V$, so that a receding star has a shorter spectrum. Hence the efficiency of the method depends critically on the dispersion law of the spectrograph. A convenient measure of this efficiency is the ratio e of the change in length to the greatest displacement measurable on a calibrated spectrum with the same dispersion variation. This ratio is given by

$$e=(K_R\lambda_R-K_V\lambda_V)/K_R\lambda_R \text{ when } K_R\lambda_R>K_V\lambda_V \text{ (gratings and grating prisms)}, \qquad (6)$$

$$e=(K_V\lambda_V-K_R\lambda_R)/K_V\lambda_V \text{ when } K_R\lambda_R<K_V\lambda_V \text{ (simple and compound prisms)}. \qquad (7)$$

* E. C. Pickering, *H.C.O. Annals*, **26**, xxi, 1891.
† J. S. Plaskett, *Dom. Obs. Pub.*, **1**, 180, 1914.
‡ A. Orbinsky, *Ast. Nach.*, **138**, 9, 1895.

Table II lists values of e for some different types of dispersion law, for the spectral range $H\alpha$ to $H\delta$.

TABLE II

Efficiency of the length of spectrum method

	$e(H\alpha$ to $H\delta)$
Light flint prism (Jena glass LF 1)	0·65
Dense flint prism (Chance glass 617366)	0·70
Dense Barium Crown prism (Chance glass 623562)... ...	0·66
Zenger direct-vision prism (Chance glasses 617366, 623562)	0·76
Simple grating	0·37
Direct-vision grating prism (Jena glass LF 1)	0·30

The effect of this limited efficiency is to increase the random error by a factor $1/e$. We have next to consider that the length method yields absolute velocities indirectly, by inter-comparison of the velocities of two stars, one of which has a well-determined slit velocity. If the change in length of the spectrum of the standard star is δL, then the difference in length of the two spectra, which is the quantity actually measured, is

$$L-l=\delta L-\delta l=(K_R\lambda_R-K_V\lambda_V)(V-v)/c; \qquad (8)$$

V being the velocity of the standard. The effect of this indirect procedure is to increase the random error by $\sqrt{2}$.

The accuracy of the length method is further impaired by the fact that the velocity determinations rest on the measurement of relatively few lines. If n pairs of stellar and comparison lines are available on a slit spectrum, and n' pairs of stellar lines are used in the length method, the error of the latter method will exceed that of the former by a factor $g=(n/n')^{\frac{1}{2}}$. The use of four pairs of lines should be practicable on panchromatic plates. If we assume an average value of 12 for n, g will have the value $\sqrt{3}$. The accidental error of the length method is therefore

$$E'=\sqrt{2}gE/e. \qquad (9)$$

The only experimental results with which we can compare this expression are Plaskett's measures * on α Orionis, spectral type M, with a dispersion of 30 A./mm. On setting $E=1{\cdot}8$ from equation (4), and $e=0{\cdot}5$, an accidental error of 8·8 km./sec. is predicted. Plaskett compared his values of the velocity on three occasions with the known velocity from slit spectra, making allowance for variations in orbital velocity. He found residuals $+2{\cdot}1$, $-2{\cdot}9$, $-13{\cdot}2$. The probable error calculated in the ordinary way from this exceedingly fragmentary material is 5·3. We must decide whether the difference between the predicted 8·8 and the observed 5·3 is significant. Reference to "Student's" t distribution tables † for small samples shows that the chances against the difference being fortuitous are about 3 : 2. There is therefore no significant difference between prediction and experiment.

1.22. *The Reversion Method.*—This method was also suggested by Pickering ‡ and was subjected to very careful experiment by Schwarzschild, with particular reference to the corrections to be applied to the spectra of non-axial stars. The essence of this method consists in the use of pairs of neighbouring spectra of the

* *Loc. cit.*

† R. A. Fisher, *Statistical Methods for Research Workers*, p. 174, 1946.

‡ E. C. Pickering, *H.C.*, **13**, 1896.

same star, with opposed directions of dispersion. These pairs may be obtained by a double exposure; the reversal of dispersion is achieved either by rotating the prism through 180°, or by reversing the telescope and prism as a single unit, and inverting the plate holder, the procedure actually followed by Schwarzschild. Alternatively, a single exposure may be used, during which the objective is covered by a pair of direct-vision prisms, following Comstock's suggestions.* Whatever method is adopted, the exposure must be twice that required for the length of spectrum method. The pairs of spectra yield, in the first place, relative velocities in a manner which the following treatment, a simplification of that given by Schwarzschild, will make plain.

Consider the direct and reversed spectra of two stars, one a standard star with known velocity V, the other a star of unknown velocity v. Let the coordinates of a particular line, say $H\gamma$, in the direct and reversed spectra of the standard, be X, X' respectively. Let the corresponding coordinates for the other star be x, x'. Let the position which this line would occupy, were no radial motion present, be X_0, X_0', in the standard star, x_0, x_0', in the other star. The last-named four positions are not observed, and are shown in Fig. 1 by dotted lines.

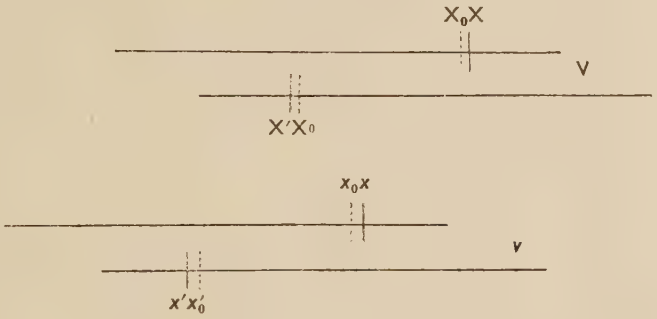

FIG. 1.—*Theory of the Reversion Method.*

The distances actually measured are

$$L = X - X' = (X_0 - X_0') + 2(X - X_0), \tag{10}$$

$$l = x - x' = (x_0 - x_0') + 2(x - x_0). \tag{11}$$

If the effects of field distortion are neglected, $(X_0 - X_0') = (x_0 - x_0')$. Furthermore, the right-hand terms $2(X - X_0)$, $2(x - x_0)$ are twice the Doppler shifts. Hence by subtraction,

$$L - l = 2K\lambda(V - v)/c, \tag{12}$$

where the notation of equation (8), to which (12) corresponds, has been reintroduced.

The most striking feature of this result is that the quantity measured is twice the Doppler shift, and that consequently the efficiency e of the method, in the sense earlier defined is 2. A further and more fundamental advantage of the method is that each line pair provides an independent velocity value, and in this respect the method is equivalent to the slit spectra method, and so $g = 1$. In calculating the error, it will however be necessary to retain the factor $\sqrt{2}$ introduced by the relative character of the measures. Consequently equation (9)

* G. C. Comstock, *Ap. J.*, **23**, 148, 1906.

holds good also for the reversion method, but with the new values of g and e, so that $E' = E/\sqrt{2}$.

This prediction is to be compared with Schwarzschild's experiment.* Schwarzschild determined radial velocities of about 30 stars in two fields, one in the neighbourhood of α Cygni, the other in the Hyades. He estimated his random error at about 7 km./sec. but this estimate is based largely on intercomparisons of velocities obtained from different lines. The situation was complicated for him by the inadvertent inclusion of a number of stars of variable velocity. With the help of modern slit-velocity measures it is possible to make a more critical evaluation of his errors. To do this it is necessary to reject 17 stars, 12 of which are known to have variable velocities, and five have no reliable slit velocities. Schwarzschild's use of the line 4272·7, produced by a *Nd* filter, in his reduction of the reversion experiments on the Cygnus field, make it necessary to exclude from this field two more stars of spectral type K, in which the *Nd* line blends with *Fe* 4271·8. The data for the remaining stars are assembled in Table III.

TABLE III

Revised Results of Schwarzschild's Reversion Experiments

	B.D.	Sp. type	Slit v	Schwarzschild Plate	Schwarzschild v	Schwarzschild Plate	Schwarzschild v
Taurus field	15°639	F	39	1593	57	1937′	52
	15°636	A	24		34		58
	13°690	A	39		5		25
	14°697	G	32		24		22
	17°719	A	36		49		30
	17°714	A	38		46		27
Cygnus field	46°2977	A	−22	1824	−21	1853	−28
	45°3233	B	−15		6		−13
	(55 Cygn.)	B	− 7		−20		−16
	46°3067	B	−15		−14		−31
	(56 Cygn.)	A	−22		−24		−23

The dispersion was about 40 A./mm. The predicted value of E' for early type according to (3) and (9) is 4·0, in satisfactory agreement with the internal probable error of 5·9, calculated from the last two columns of Table III. Comparison of Schwarzschild's results with the slit values gives an external probable error of 9·0. This large error is certainly due in part to the unfortunate choice of the variable velocity star θ_1 Tauri as one of the standards. It also reflects the systematic errors to which the reversion method is exceptionally subject, on account of the corrections that must be applied for the very large field distortions of ordinary prisms.

1.23. *The Absorption Filter Method.*—The use of the *Nd Cl* filter, which makes this method practicable, was first proposed by Wood † and in this form the method has been the subject of several researches, the most recent being those of Bok and McCuskey.‡ For a full account of the history of the subject, reference must be made to Millman's article and bibliography.§ The absorption filter method has an efficiency $e = 1$, since the complete Doppler shift is measured by reference

* *Loc. cit.*

† R. W. Wood, *Ap. J.*, **31**, 376, 1910.

‡ *Loc. cit.*

§ P. Millman, *Jn. R.A.S. Canada*, **25**, 293, 1931.

to the undisplaced *Nd* line 4272·7. This line is the best available, but is far from ideal, since it is about 3 A. wide, has a central intensity of 50 per cent, and blends with *Fe* 4271·8 in stars of spectral type G and later.

To calculate the value of E' for the method we have again to consider the effect on the probable error of the number of lines measured. The position here is that n' stellar lines can be measured, but only one good reference line. If the probable error in plate position determination of a stellar line is a', the probable error of these n' determinations relative to the *determined* position of the *Nd* line is $a'/\sqrt{n'}$. The error of measurement, b', of the *Nd* line will have its full effect on each spectrum measured. The probable error will therefore be $(b'^2+[a'^2/n'])^{\frac{1}{2}}$. In slit spectra, if a and b are probable errors of star and comparison lines respectively, the error for each pair is $(a^2+b^2)^{\frac{1}{2}}$, and for n pairs the error is $(a^2+b^2)^{\frac{1}{2}}/n^{\frac{1}{2}}$. The value of the factor g is consequently:

$$g=\left\{\frac{b'^2+(a'^2/n')}{(b^2+a^2)/n}\right\}^{\frac{1}{2}}. \qquad (13)$$

Neglecting the difference in the errors due to the type of line used and the definition of the spectra, and setting $n=12$ as before, we find that g falls from 3 to 2·55 as n' increases from 2 to 12. The *Nd* method is, like the other methods, comparative, so that the factor $\sqrt{2}$ must be introduced once more. The value of E' is consequently given as before by (9), with the appropriate values of e and g.

In comparing this prediction with the observational results of Millman, and of Bok and McCuskey, we must note that they calculate their errors by the intercomparison of velocities derived from spectra, all of which have been calibrated by the same standard spectra. Under these conditions the errors of the standard do not influence the internal probable error, but become systematic. In predicting their internal error, the factor $\sqrt{2}$ must therefore be omitted.

Millman * determined velocities of ten early type stars, using a dispersion of 230 A./mm. He used three stellar lines, and attempted to measure *Nd* C as well as *Nd* A. His probable error per plate was ±67 from Gaertner measuring machine determinations, and ±45 from Hartmann spectrocomparator measures. The predicted value gE is 59. The agreement is quite good, and Millman's results support his contention that the use of the comparator gave more consistent measurements on the diffuse *Nd* line.

Bok and McCuskey measured two stellar lines. For the Taurus field, in which late type stars predominate, the dispersion used (90 A./mm.) leads to a predicted error of ±14 km./sec., and for the early type stars of the Cygnus field ±29 km./sec. Bok and McCuskey made five subdivisions of spectra according to quality, and found probable errors ranging from 6·4 to 14·5 for the Taurus field, and from 12·9 to 41·5 for the Cygnus field. The subdivision of material, particularly for the Taurus field, is a refinement of doubtful value, since the samples resulting are too small to lend themselves to reliable statistical treatment. With this reservation the general agreement between prediction and experiment is reassuring.

The introduction of the *Nd* cell into the optical train at a short distance from the plate introduces another important source of accidental error. Schwarzschild, Millman, and Bok and McCuskey all used cells with plate-glass walls. Schwarzschild remarked that the introduction of the cell produced no sensible deterioration

* P. Millman, *H.C.*, **357**, 3, 1930.

of the spectra. Small deviations from planeness in the cell walls, in the case of a cell placed fairly close to the plate, would not however be expected to produce a badly defined spectrum, but rather to produce local displacements in line position. If x is the distance between the nearer cell wall and the plate, i the small angle between two elements of surface of this wall, in front of different regions of the same spectrum, the relative displacement of lines in these two regions will be $xi(n-1)$, where n is the refractive index of the cell wall. For example, in Millman's work, x was 3 cm. If we set $n=1{\cdot}5$, $i=10^{-4}$ radians (about $\frac{1}{3}$ minute, a low value for plate glass), the displacement amounts to 0·0015 mm., corresponding to a velocity shift of 23 km./sec. at 4500 A. Schwarzschild's much shorter filter-to-plate distance (a few mm.) and higher dispersion, render his work less open to criticism on this score. The error in Bok and McCuskey's work, assuming that they used the same filter-to-plate distance as Millman, would be 10 km./sec. Although the empirical determination of the variation of dispersion over the plate may have diminished the importance of the effect, it may still be invoked to account for the wide discrepancy between the form of the dispersion variation found by them and that predicted by Schwarzschild from geometrical theory.

1.3. *Comparison of the Slitless Methods.*—In the preceding section the accidental error E' of each of the slitless methods has been related to the slit spectrograph error E by an expression of the form $E'=\sqrt{2}gE/e$, where g and e depend upon the method. Though the observational data against which this expression has been tested are somewhat meagre, the experiments cover a very wide range of conditions, leading to probable errors varying from 6 to 67 km./sec. The general agreement between prediction and experiment in all cases is therefore very reassuring, and enables a comparison to be made of the different methods under equivalent conditions. With a given telescope and exposure time, the dispersion that can be employed is limited by the faintness of the stars under investigation. If in a particular case the limit is 100 A /mm. for the length and absorption cell methods, it will, for obvious reasons, be 200 A./mm. for the reversion method. Using (3) and (4) and the values of g and e given in Table IV, which correspond to rather favourable conditions, we may predict the errors for this example. The values so calculated for early and late type stars occupy the last two columns of Table IV. The errors are in km./sec., and refer to single plates.

TABLE IV

Probable errors in slitless spectra

Method	d A./mm.	g	e	E' (early type)	E' (late type)
Length	100	$\sqrt{3}$	0·66	37	18
Reversion	200	1·0	2·0	14	7
Absorption	100	2·6	1·0	37	18

From this table we must draw the following conclusions.

(*a*) The reversion method alone should be capable of furnishing useful velocities from a single plate for *all* stars, provided the dispersion is not less than 100 A./mm.

(*b*) The length method should provide useful velocities for later type stars from a small accumulation of plates, provided the dispersion exceeds 100 A./mm. The method is hardly capable of application to stars of early type.

(*c*) Though the error of the *Nd* method is the same as that of the length method, it is inapplicable to the bulk of late type stars on account of blending, and to early type stars on account of the large errors. It may however be used with stars of type F.

Part II. Systematic Errors of Existing Methods

2.1. *The Sources of Systematic Error.*—The considerations which justify the toleration of a random error of ± 7 to ± 8 km./sec. in the statistical use of line-of-sight velocities do not apply to systematic errors, which must of course be eliminated. The experiments of Schwarzschild, of Millman, and of Bok and McCuskey all reveal the presence of systematic errors of several km./sec. The three main sources of systematic error are temperature variation, flexure and field distortion. Attention has, in the past, been largely confined to the last of these sources of error in connection with slitless velocity measures. Since, however, reliable results were not obtained from slit spectra until the need for special precautions to eliminate flexure and temperature variation was realized, it is essential to consider the rôle of these effects in slitless spectra.

2.11. *Flexure Effects.*—J. S. Plaskett* gives 7 km./sec. as a conservative estimate of the flexure displacement occurring during a 1-hour exposure in a slit spectrograph of older design. Since objective prism systems are only supported at one point, they are subject to mechanical strains similar to those which produced these flexures. The situation is further aggravated by the lower dispersion, and by the difficulty of accurate guiding with the objective prism in position. In the double-exposure form of the reversion method used by Schwarzschild, this flexure is liable to have its full effect. The part played by flexure in the other methods is less serious, since the conditions are analogous to slit-spectrograph experiments in which comparison exposures are well distributed throughout the star exposure. There is, however, no justification for resting satisfied with a mechanical rigidity inferior to that of a modern slit spectrograph of the same dispersion.

2.12. *Temperature Effects.*—In order to estimate the magnitude of the temperature effect, we shall calculate, for each method, the effect of a temperature change $T-t$ between a calibrating exposure on a standard star and a subsequent exposure. The error thus calculated represents, of course, a maximum effect, which may be diminished by appropriate methods of reduction.

(*a*) Length of spectrum method. The length of the spectrum of the standard star between λ_1 and λ_2 is

$$l = fA(n_1 - n_2), \tag{14}$$

where f is the focal length of the camera, n_1, n_2 the refractive indices of the prism at λ_1, λ_2, and A is the prism angle, assumed small. The difference in length between this spectrum and that of the star subsequently examined, is due to two physically independent effects, viz.: a change in temperature $T-t$ and a change in velocity $V-v$. Considering only small changes, we may therefore write

$$\Delta l = \left(\frac{\partial l}{\partial v}\right)_t \Delta v + \left(\frac{\partial l}{\partial t}\right)_v \Delta t. \tag{15}$$

* J. S. Plaskett, *Report of the Chief Astronomer, Dominion Observatory, Ottawa*, 92, 1907.

For finite changes $(V-v)$, $(T-t)$ we have, correspondingly,

$$L-l=\int_v^V\left(\frac{\partial l}{\partial v}\right)_t dv+\int_t^T\left(\frac{\partial l}{\partial t}\right)_v dt. \tag{16}$$

Now $(\partial l/\partial v)_t$ is essentially proportional to dispersion, which is practically constant over the exceedingly small spectral region involved in a velocity shift. Similarly, we may neglect the variation in the temperature coefficient of n over a few degrees. We may therefore integrate (16) and obtain finally

$$L-l=(\partial l/\partial v)_t(V-v)+(\partial l/\partial t)_v(T-t). \tag{17}$$

The first term on the right of (17) is the change in length at constant temperature, given by (8). The second term is obtained by partial differentiation of (14). Making these substitutions, we find

$$L-l=(K_1\lambda_1-K_2\lambda_2)(V-v)/c+fA\left[\left(\frac{\partial n_1}{\partial t}\right)_v-\left(\frac{\partial n_2}{\partial t}\right)_v\right](T-t). \tag{18}$$

Noting that $K=fA\,.\,dn/dt$, (18) may be written

$$L-l=\frac{1}{c}(K_1\lambda_1-K_2\lambda_2)\{(V-v)+c\frac{\left[\left(\frac{\partial n_1}{\partial t}\right)_v-\left(\frac{\partial n_2}{\partial t}\right)_v\right](T-t)}{\lambda_1\left(\frac{\partial n_1}{\partial\lambda}\right)_t-\lambda_2\left(\frac{\partial n_2}{\partial\lambda}\right)_t}, \tag{19}$$

which on comparison with (8) shows that a temperature change $T-t$ will be interpreted as a velocity δv, where

$$\delta v=\frac{c\left\{\left(\frac{\partial n_1}{\partial t}\right)_v-\left(\frac{\partial n_2}{\partial t}\right)_v\right\}(T-t)}{\lambda_1\left(\frac{\partial n_1}{\partial\lambda}\right)_t-\lambda_2\left(\frac{\partial n_2}{\partial\lambda}\right)_t}. \tag{20}$$

The other methods may now be given a more summary treatment.

(*b*) The reversal method. In this method the effect of a temperature change $T-t$ will be to shift the rest positions of the lines, x_0, x_0', by an amount $fA\,(dn/dt)\,(T-t)$ in opposite senses. The formerly equal quantities X_0-X_0', x_0-x_0' of (10) and (11) will now differ by $2fA(dn/dt)(T-t)$. (12) must therefore be replaced by

$$(L-l)=2K\lambda(V-v)/c+2fA(dn/dt)(T-t). \tag{22}$$

After substitution for fA and rearrangement, this becomes

$$(L-l)=(2K\lambda/c)\{(V-v)+(c/\lambda)(d\lambda/dn)(dn/dt)(T-t)\}. \tag{23}$$

Comparing this with (12) we see that the effect of ignoring the temperature change will be to introduce an error in velocity

$$\delta v=c(d\lambda/dn)(dn/dt)(T-t)/\lambda. \tag{24}$$

(*c*) Absorption cell method. Here the change in distance between a stellar line λ_1 and the reference line λ_2 will be entirely attributed to the velocity displacement of the stellar line. Hence

$$fA\left(\frac{dn_1}{dt}-\frac{dn_2}{dt}\right)(T-t)=K_1\lambda_1\delta v/c, \tag{25}$$

so that

$$\delta v=c\left(\frac{dn_1}{dt}-\frac{dn_2}{dt}\right)(T-t)/\lambda_1(dn_1/d\lambda). \tag{26}$$

Since f and A do not appear in the formulae (20), (24), (26) for δv, the errors can be calculated from knowledge of the glass constants alone. Table V gives the data for, and the results of, this calculation for a typical light flint glass and a temperature change $T-t$ of 1 deg. C. The errors are in km./sec. The particularly high sensitivity of the reversion method to temperature effects is noteworthy.

TABLE V

Contribution of Temperature Effects to Systematic Errors

Line	C	D	F	G′	Remarks
λ	6563	5893	4861	4341	
n	1·56911	0·57298	0·58298	0·59055	Jena glass tables (glass LF 1)
$dn/d\lambda$	0·52	0·65	1·32	$1{\cdot}67\times10^{-5}$	Estimates from disp. curve
dn/dt	0·225	0·261	0·334	$0{\cdot}407\times10^{-5}$	Smithsonian Physical Tables
δv (length)	14·3	12·8			Refers to intervals C–G′, D–G′
δv (rev)	19·8	20·5	15·6	16·8	
δv (abs)	16·0	11·0	3·4		Refers to intervals C–G′, D–G′, F–G′

Bok has suggested * that modern reflecting telescopes should be used in slitless velocity determinations. The change in focal length of glass mirrors with temperature and the consequent alteration of the scale of the spectra would produce an additional source of temperature error.

2.13. *Field Distortion Effects.*—The plate coordinate differences x_1-x_2, y_1-y_2 between the images of two stars in light of any particular wave-length, produced after refraction in a prism, differ from the coordinate differences $\xi_1-\xi_2$, $\eta_1-\eta_2$ of the star images of the same field, produced without the prism in position. If the x axis contains the direction of dispersion, we may write

$$x_1-x_2=\xi_1-\xi_2+G(\xi,\eta). \qquad (27)$$

where G is a function of the plate coordinates, whose properties have been investigated by Schwarzschild.† This "distortion" function has a slight dependence on wave-length, and the difference of its value for two wave-lengths in one and the same spectrum produces a small relative shift of the lines, which constitutes the "variation of dispersion" over the field, and has to be determined in all methods. In the reversion method, however, the distortion produces in addition a relative shift of order of magnitude $2G$ between direct and reversed spectra, a shift which may amount to *several millimetres*. The practical difficulty of making proper allowances for this shift constitutes the great weakness of the reversion method as normally proposed.

The conclusion that one must inevitably draw is that the reversion method is subject to all three forms of systematic error in an aggravated degree, in striking contrast to its relative freedom from accidental errors, indicated in Part I. No serious prospects can be held out for the slitless methods, until all the factors responsible for the systematic errors are properly controlled.

* B. J. Bok, *Pop. Ast.*, **52**, 83, 1944.

† *Loc. cit.*

2.2. *The Elimination of Systematic Error.*—Two remedies are proposed for the state of affairs outlined above. The first is to diminish the effect of temperature and flexure by deriving results from a single exposure. The second is to eliminate the errors at their source by suitably designed slitless spectrographs.

2.21. *A single plate method of reduction.*—It is clear what from has been said, that systems of reduction which require two exposures are subject to the full weight of the effects of temperature and flexure. The "standard" plates which necessitated a second exposure in the work of Millman, and of Bok and McCuskey, served a double purpose, first the determination of the variation of dispersion, and secondly, the provision of stars of known standard velocity. The fewness of stars with well-determined slit velocities, and the disparity in magnitude between these and the field stars, make it difficult to secure a standard star on each plate. It would be possible, however, using only one plate, to determine the velocities relative to one or more stars, of which the velocities could be subsequently determined by slit spectra, provided, however, that the dispersion variation can be allowed for. Schwarzschild has shown that the variation of dispersion can be represented as a simple expansion or contraction of the scale of the spectrum. What is required, therefore, is a method of comparing two spectra which, apart from velocity shifts, differ only in scale. The following paragraphs will describe a method of this kind, which bears some resemblance to that employed by Bok and McCuskey.*

For simplicity we shall consider the determination of a velocity by the *Nd* cell method, using the stellar lines $H\gamma$, $H\delta$. Denote the distances $H\gamma - Nd$, $Nd - H\delta$ in the spectrum of the unknown star by γ, δ, and the distances that would be measured in the absence of radial velocity by γ_0, δ_0. Let the corresponding distances on the standard, after correction to zero velocity, be γ_s, δ_s. The velocity v of the unknown star is given by

$$(\gamma - \gamma_0) = K_\gamma \lambda_\gamma v/c, \tag{28}$$

where K and c have the usual meaning, or by a corresponding equation in δ. The problem is to determine γ_0. If no scale differences were present this would be equal to γ_s. As it is, we must set $\gamma_0 = m\gamma_s$, m being a scale factor which will have the value

$$m = \frac{\text{Rest length of star spectrum}}{\text{Rest length of standard spectrum}} = \frac{\gamma_0 + \delta_0}{\gamma_s + \delta_s} = \frac{\gamma + \delta - \Delta l}{\gamma_s + \delta_s}, \tag{29}$$

Δl being the change in length due to the velocity v, given by (5). Substitution for γ_0 in (28) gives

$$\gamma - \frac{\gamma_s(\gamma + \delta - \Delta l)}{\gamma_s + \delta_s} = K_\gamma \lambda_\gamma v/c, \tag{30}$$

and after substitution from (5) and solving the resulting equation for v,

$$v = \frac{\gamma - \gamma_s\left(\dfrac{\gamma + \delta}{\gamma_s + \delta_s}\right)}{\dfrac{K_\gamma \lambda_\gamma}{c} - \dfrac{1}{c} \cdot \dfrac{(K_\gamma \lambda_\gamma - K_\delta \lambda_\delta)}{\gamma_s + \delta_s}}. \tag{31}$$

The essence of the method consists in the use of the fact that the change in length of the spectrum over the length measured is very much shorter than the shift relative to the *Nd* line. This length, with the small velocity correction

* *Loc. cit.*

indicated, provides in consequence a measure of dispersion variation, precisely at the positions on the plate where this knowledge is required, and subject to the same conditions of temperature and flexure which influence the velocity measures. This reduction process can also be applied to the reversion and length methods. In the latter method one must use a considerably shorter length for determining the dispersion variation than for the actual velocity measures.

2.22. *The Advantages of Slitless Spectrographs.*—Though a reduction process such as that outlined would eliminate some of the grosser systematic errors, it will not by itself suffice, but must be supplemented by actual control of the sources of error, in the manner which has been found necessary with slit spectra. In this connection, the advantages of slitless spectrographs over objective prisms call for special emphasis, and will be considered under the following headings.

(*a*) Temperature. The necessary control of prism temperature to a small fraction of a degree is all but impossible with large objective prisms. In slitless spectrographs the negative collimator and camera lenses enclose the prism in a small chamber which may readily be temperature controlled. Moreover, the scale of the spectra is determined by the focal length of the camera lens, so that the use of reflecting telescopes is no longer barred by the variation of focal length with temperature. Refocussing during exposure would best be affected by moving the whole spectrograph with respect to the mirror.

(*b*) Field distortion. It is possible to design large-angled compound prisms which wholly eliminate field distortion for one wave-length, and reduce variation of dispersion (see Part III). For obvious reasons, such prisms can only be constructed for slitless spectrographs.

(*c*) Flexure. Slitless spectrographs, on account of their lightness and compactness, can be made, by the ordinary two-point support system, as free from mechanical flexures as slit spectrographs.

(*d*) Guiding Errors. In slitless spectra, the star itself replaces the normal slit. Consequently, one must eliminate not only the displacements due to spectrograph flexures, but also the analogous displacements produced by guiding errors. These errors arise from defects of mounting, and flexures of the telescope tube, and can only be removed by accurate guiding on the star image which is to be dispersed. Such guiding is not possible in objective prism systems, but may readily be achieved with slitless spectrographs.

Besides affording a means of eliminating the all-important systematic errors, the use of slitless spectrographs would permit a greater flexibility of experimental procedure, which would lead to a further reduction of errors. For example, in the absorption cell method the use of a small cell with optically flat walls, placed in the collimated beam, would eliminate the displacements produced by the cell walls. The production of the reversed spectra required for the reversion method, either by rotating the prism, or by Comstock's method, can only be successfully achieved by the use of the small direct-vision prism systems rendered possible by slitless spectrographs. The numerous solid advantages thus promised seem to indicate that slitless spectrographs must supplant objective prisms in the determination of radial velocity.

Part III. A New Form of Stellar Image Method

3.1. *Pickering's Experiment.*—The possibility of using the undispersed star image as a point of reference for the measurement of velocity shifts was considered

by Pickering.* He performed an experiment in which a small achromatic prism, placed near the edge of a telescope objective, produced deviated star images, which coincided with the spectra of the stars produced by the objective prism. Now it is clear from the discussion of systematic errors in Part II, that a method of this kind, besides being subject to errors arising from flexure and from temperature change, is, like the reversion method, particularly subject to those field distortion errors, which involve the distortion function G in its entirety, and not merely its variation with wave-length. We need no further consideration than this to account for the complete failure of Pickering's experiment. Certain other errors, extraneous to the method as such, were introduced by Pickering's optical system, including the effects of secondary dispersion and diffractional broadening of the star image by the achromatic prism, and line displacement due to the asymmetrical location of the small prism, of the same type as that observed in Hartmann focussing tests.†

The precision with which a star position can be measured is at least equal to that of the measurement of lines in slitless spectra, since these spectra are subject to the same atmospheric and instrumental conditions which determine the definition of stellar images. There appears, therefore, to be no reason why the accidental errors of this method should exceed those of the absorption cell method, in which one is restricted to a single reference line of poor quality. An attempt will therefore be made to propose the method in a new form, which aims both to avoid the principal systematic errors and also those errors adventitiously introduced by Pickering's optical system.

3.2. *The Essentials of the New Method.*—The essence of the new method is as follows. Into the collimated beam of a temperature-controlled slitless spectrograph a direct vision compound prism is introduced (Fig. 2). This

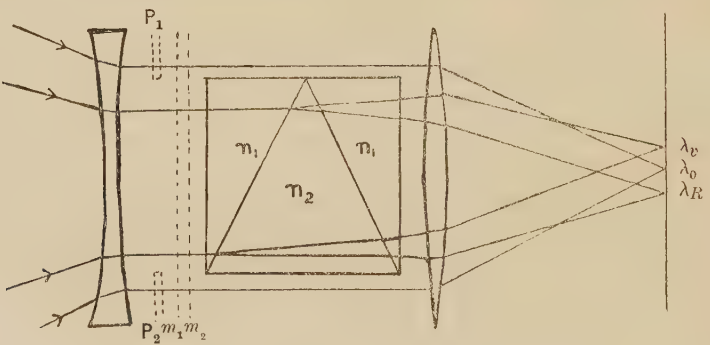

FIG. 2.—*The Stellar Image Method* (*Diagrammatic*).

prism, in virtue of special design, completely eliminates field distortion effects for the undeviated wave-length, which is determined only by the glass constants of the components. The prism does not occupy the whole aperture of the system, but leaves free an outer annulus, through which undispersed light from any star may pass and produce a star image coincident with λ_0, the undeviated wave-length in the spectrum of the star. To measure the velocity of the star, the undispersed star image is treated as a spectral line of wave-length λ_0, and used

* E. C. Pickering, *H.C.O. Annals*, **26**, xxi, 1891.
† J. Hartmann, *Zeits. f. Instrkde.*, **20**, 47, 1900.

as a reference line in the same way as the *Nd* line, the reduction being carried out by the method explained in 2.21.

3.3. *Prism Design.*—The simplest form of prism which eliminates field distortion for one wave-length is that proposed by Zenger.* The Zenger prism consists of two right-angled prisms, geometrically identical in construction, in contact along their hypotenuse faces, so that the common principal section of the combination is rectangular. The dispersion curves of the prism materials have different slopes, and intersect in the visible region, the wave-length of intersection defining the undeviated colour. For light of this wave-length, the combination will behave as a homogeneous, parallel-sided glass plate. Light of this wave-length, which is determined by the optical properties of the glasses alone, will pass through the combination undeviated, whatever the angle of incidence. For this wave-length, therefore, field distortion is completely absent.

Prisms of this type intended for laboratory work usually have one liquid component, a circumstance which would be disadvantageous in radial velocity work on account of the high temperature coefficients of refractive index of liquids. We must therefore ascertain whether it is possible to construct such a prism from available glasses, with sufficient dispersion for accurate work. To do this, we first require an approximate expression for the dispersion of a Zenger prism. Consider a ray of light incident normally on the first face of a Zenger prism of angle a. Let the refractive indices of the components for wave-length λ be n_1, n_2. The deviation of this ray at the slanting interface of the components will be δ, and the emergent ray will make an angle δ' with the incident ray. These quantities are related by the equations

$$\sin \delta' = n_2 \sin \delta, \tag{32}$$

$$n_1 \sin a = n_2 \sin (a+\delta). \tag{33}$$

Substituting (32) in (33), and expanding,

$$n_1 \sin a = n_2 \sin a \cos \delta' + \cos a \sin \delta', \tag{34}$$

or, since δ, δ' are small,

$$\delta' = (n_1 - n_2) \tan a. \tag{35}$$

Since the deviation is zero for λ_0, (35) represents the angular dispersion between λ and λ_0. A typical selection of favourable pairs of glasses from the Chance Catalogue is given in Table VI.

TABLE VI

Glass pairs for Zenger Prisms

D.Fl.	D.Ba.Cr.	Undeviated λ	D.Fl.	D.Ba.Cr.	Undeviated λ
605380	618557	4000	620361	621572	5750
617366	623562	4500	617366	616552	6200
620361	623562	5100	620361	618557	6750

These glasses give, according to (35), dispersions of the order of 75 A./mm. at $H\gamma$ at one metre with $a = 45°$. It is clear that Zenger prisms of adequate dispersion can be constructed for use in slitless spectrographs, but not for large objective prisms, with a wide range of undeviated wave-lengths.

* K. W. Zenger, *Zeits. f. Instrkde.*, **1**, 263, 1881.

The simple Zenger prism has but one disadvantage for radial velocity work, namely, that it produces rather large variation of dispersion. If the successive angles of incidence and refraction in a Zenger prism of angle a are $i_1 \ldots . i_6$, the exact expression for the dispersion is

$$\frac{di_6}{d\lambda} = \frac{\sin a}{\cos i_4 \cos i_6}\left(\frac{dn_1}{d\lambda} - \frac{\cos i_5}{\cos i_2}\frac{dn_2}{d\lambda}\right), \tag{36}$$

an expression which may be derived as a particular case of the theory treated, e. g. by Herman.* Since i_4 is of the same order of magnitude as a, provided $a \gg i_1$, the variation of dispersion will in practical cases be determined chiefly by the variation in i_4. Under these conditions (36) may be approximated to the form

$$di_6/d\lambda = \text{const.}/\cos i_4. \tag{37}$$

To take an example, in a 60° Zenger prism, a variation of 2° in i_4 will alter the dispersion by about 6 per cent. A simple modification, however, eliminates this defect. Consider two similar Zenger prisms placed back-to-back, to form the triplet prism of Fig. 2. If the angle of refraction at the new slanting interface is i_4', the contribution of the slant faces to the dispersion becomes

$$di_6/d\lambda = \text{const.}/\cos i_4 \cos i_4', \tag{38}$$

in which small increments in i_4 are largely offset by nearly equal decrements in i_4'. This form of prism, first introduced by Wernicke, satisfies all the requirements of the stellar image method.†

3.4. *Possible Modifications.*—Two possible lines of development may be mentioned, which would bring the method more into line with slit spectrograph procedures. The first is to replace the annular aperture by two slits, with their lengths parallel to the direction of dispersion. By covering both these slits with prisms of very small angle, P_1, P_2 in Fig. 2, producing deviations in opposite senses, and perpendicular to the dispersion of the compound prism, two star images would be obtained, one above, the other below, the spectrum at λ_0. These would resemble the double comparison lines of slit spectra, which leave the star spectrum undisturbed.

The second suggestion is to increase the number of available reference points by means of multiple reflection in a pair of partially silvered glass flats, mounted with their surfaces mutually inclined by means of a suitable spacer. The partial silvering of these flats, which are indicated by m_1, m_2 in Fig. 2, would of course extend only over the aperture for the undispersed light. The stability of this arrangement would be equal to that of a temperature-controlled étalon; a much less stringent optical tolerance is of course permissible.

3.5. *Advantages of the Method.*—There seems good reason to believe that the new method will be reasonably free from the normal systematic errors. It is also designed to avoid the peculiar difficulties of Pickering's arrangement. The annular aperture, owing to its symmetry and size, avoids the danger of diffractional broadening and focal errors. In the double-slit form, diffractional broadening and focal shifts, as well as the slight spreading due to the dispersion of the thin

* R. A. Herman, *Geometrical Optics*, p. 173, 1900.

† These properties of the Wernicke prism have been independently noted, in connection with the *reversion* method, by C. Fehrenbach (*C.R.*, **219**, 201, 1944), whose priority in this respect the author wishes to acknowledge.

prisms, will be perpendicular to the dispersion of the main prism, and therefore unimportant.

The Stellar Image method avoids the severe blending difficulties of the *Nd* method, and the experimental complications of the reversal method. Its accidental error, in the primitive form, should be at worst that predicted for the length-of-spectrum and *Nd* methods, and if the multiple image form can be realized, should rival that of the reversion procedure.

It is noteworthy that the prism system described is, on account of its high " efficiency " (see Table II), freedom from field distortion and low dispersion variation, highly suited for use with all four procedures. The simultaneous determination of radial velocity by all methods would provide a much needed direct experimental check on their relative merits. It may well prove that the economy of observing time and low accidental error obtainable by a suitable combination of methods, will put the utility of measurement of radial velocity by slitless spectrographs beyond reasonable doubt.

The author wishes finally to express his indebtedness to Professor Plaskett for his invaluable discussions and advice connected with the matter of this article.

University Observatory, Oxford:
1948 *March* 3.

Note added in proof.—Since the submission of the present article, a series of three papers has been published on the same subject by C. Fehrenbach.* Following a rather different method, Fehrenbach reaches many of the conclusions which have been drawn in the present article. The writer of the present article cannot, however, agree with the summary rejection of the length method, since this was based upon a calculation of efficiency which ignored the possible use of panchromatic plates, and the peculiarly high efficiency of Wernicke prism systems. The conclusion was also drawn in ignorance of J. S. Plaskett's results. The most important bearing of this series on the present paper is, however, the experimental vindication of the reversion method, when used with a Wernicke prism system. The successful use of a small objective prism system in these observations in no way vitiates the argument in favour of slitless spectrographs with temperature control for the continued study of the radial velocities of faint stars.

* C. Fehrenbach, *Annales d'Astrophysique*, **10**, 257, 1947; **10**, 306, 1947; **11**, 35, 1948.

THE EARTH'S CORE AND THE LUNAR NUTATION

Harold Jeffreys

(Received 1948 March 3)

Summary

The effects of fluidity of the core on the amplitude of the lunar nutation and on the period of the Eulerian nutation are discussed ; the formal solution for a rigid crust is given by Lamb and the quantitative data for the core by Bullen. The amplitude of the lunar nutation on these hypotheses would be reduced from the present theoretical value (for a rigid Earth) by about three times as much as is needed to remove the present discrepancy between theory and observation. It seems probable that this over-correction would be reduced if allowance were made also for the elasticity of the shell.

A fluid core would shorten the period of the Eulerian nutation by about 10 per cent in comparison with that for a rigid body with the same total moments of inertia.

It is well known that there is a discrepancy between the theoretical and observed values of the amplitude of the lunar nutation in latitude. The calculated value, as revised by Sir H. Spencer Jones *, is $9''{\cdot}2272 \pm 0''{\cdot}0008$ (p.e.). The observed value usually adopted is $9''{\cdot}210 \pm 0''{\cdot}008$, due to Newcomb. E. Przybyllok got $9''{\cdot}207 \pm 0''{\cdot}003$, and J. Jackson † $9''{\cdot}2066 \pm 0''{\cdot}0055$. Spencer Jones in a redetermination ‡ gets $9''{\cdot}2134 \pm 0''{\cdot}0042$. Systematic errors have been suspected in the observations. On the other hand the calculated value depends on the assumption that the Earth is a rigid body, which is certainly false, though it seems likely that the correction for elasticity is small.

The calculations of the tidal yielding of the Earth that have been made hitherto, taking account of the fluidity of the core, have proceeded by adapting the solution of Herglotz for an elastic sphere, with the properties of the core and shell different, by taking the rigidity of the core zero. This procedure appears to be invalid. The solution is a statical one, and the justification of its application to the actual Earth is that the periods of elastic vibrations are all short compared with those of astronomical disturbing forces and with the period of rotation, so that the inertia terms in the equations of motion can be neglected. But for the core it is not legitimate first to neglect inertia in comparison with the rigidity and then to put the rigidity zero. Further, the elastic solution assumes continuity of displacement at the core boundary. For a classical fluid this is not true, and in a real fluid, though there is continuity of velocity, the effect of viscosity is usually to introduce a boundary layer, where there may be rapid shearing, while most of the fluid still moves nearly according to the classical rules; in particular the normal velocity just outside the boundary layer is nearly that of the solid, so that the solution given by classical hydrodynamics may be a good approximation except close to the boundary. Lyttleton and Bondi are examining the problems of viscosity in the

* *M.N.*, **101**, 365, 1941.
† *M.N.*, **90**, 733–742, 1930.
‡ *M.N.*, **99**, 211–216, 1939.

core and have drawn my attention to a passage in Lamb's *Hydrodynamics* * in which the classical solution, taking account of inertia, is given, and this should be nearly correct. Kelvin actually pointed out in 1876 † that if an extensive part of the Earth was fluid the theoretical coefficient in the nutation would be substantially reduced; with a rigid crust, apparently of small thickness, the reduction would be by about 1 part in 23. Apparently the details of the calculation were never published, but Lamb's discussion, based on a method of Poincaré, covers the ground. Lamb gives no quantitative estimate, and the results seem to have escaped attention, but in view of the very definite evidence that now exists in favour of a fluid core the probable effect becomes a matter of considerable importance.

After various approximations of standard type Lamb finds that with a rigid shell and axes fixed in it, the components of rotation of the shell being (p, q, ω), and the disturbing couples $(L, M, 0) = \kappa(\cos\sigma t, \sin\sigma t, 0)$, p and q are the real and imaginary parts of

$$\varpi = -\frac{A_1\sigma + C_1\omega}{\Delta(\sigma)}\, i\kappa e^{i\sigma t}.$$

Here C, A are the moments of inertia of the Earth as a whole, C_1, A_1 those of the core, and

$$\frac{C_1 - A_1}{A_1} = \epsilon; \quad F^2 = A_1^2(1-\epsilon^2),$$

$$\Delta(\sigma) = \begin{vmatrix} A\sigma - (C-A)\omega & F(\sigma+\omega) \\ F\sigma & A_1\sigma + C_1\omega \end{vmatrix}.$$

The core does not move as a rigid body, but its motion is expressed by variables p_1, q_1, which are the real and imaginary parts of

$$\varpi_1 = \frac{F\sigma}{\Delta(\sigma)}\, i\kappa e^{i\sigma t}.$$

When, however, the ellipticity of the core is small p_1, q_1 are nearly the differences between the angular velocities of the core and shell.

The free periods are given by $\Delta(\sigma) = 0$. If $A_1 = C_1 = 0$, the free period is given by

$$\frac{\sigma}{\omega} = \frac{C-A}{A},$$

as we should expect, since the conditions then reduce to those of the Eulerian nutation of a rigid body. In general we can write

$$\Delta(\sigma) = \{A\sigma - (C-A)\omega\}A_1\{\sigma + (1+\epsilon)\omega\} - A_1^2(1-\epsilon^2)\sigma(\sigma+\omega).$$

Treat $(C-A)/A$ and ϵ, and therefore σ/ω, as small quantities of the first order, and write the equation as

$$A\sigma - (C-A)\omega = \frac{A_1(1-\epsilon^2)\sigma(\sigma+\omega)}{\sigma + (1+\epsilon)\omega} = \frac{A_1\sigma}{1+\epsilon} + O(\epsilon^3, \sigma^3).$$

Then

$$\frac{\sigma}{\omega} = \frac{C-A}{A - A_1/(1+\epsilon)} + O(\sigma^3) = \frac{C-A}{A-A_1} + O(\epsilon^2).$$

---

* Pp. 724–727 of 1932 edition.

† *Math. and Phys. Papers*, **3**, 323; *B.A. Report*, ii, 1, 1876.

Thus the period of the free nutation is shortened by fluidity of the core in the ratio $(A-A_1)/A$. This result was noticed by Hough.* It is remarkable that, while elasticity lengthens the period, partial fluidity should shorten it. The explanation is seen when we examine ϖ_1, which is nearly $-\varpi$ when σ/ω is small. The oscillations hardly communicate themselves to the core at all, so that the inertia of the core plays a negligible part in determining the period.

For couples about axes nearly fixed in space σ is nearly $-\omega$. Put

$$\sigma = -\omega + n,$$

with n/ω small. Then

$$\varpi = \frac{n+\epsilon\omega}{\epsilon C\omega^2 + \{C - A\epsilon - A_1(1-\epsilon^2)\omega n - \{A - A_1(1-\epsilon^2)\}n^2}\, i\kappa e^{i\sigma t},$$

and $|\varpi_1|$ is large compared with $|\varpi|$. Let ϖ reduce to ϖ_0 when $A_1 = 0$, and neglect $A_1\epsilon^2$. Then

$$\frac{\varpi}{\varpi_0} = \frac{\epsilon C\omega^2 + (C - A\epsilon)\omega n - An^2}{\epsilon C\omega^2 + (C - A\epsilon - A_1)\omega n - (A - A_1)n^2}$$
$$= \left\{1 - \frac{A_1(\omega n - n^2)}{(C\omega - An)(\epsilon\omega + n)}\right\}^{-1}.$$

This reduces to 1 when $n = 0$. Thus the effect on the precession should be inappreciable. But for the nutation $n/\omega = -1/6800$. From Bullen's calculation †

$$\tfrac{2}{3}A_1 + \tfrac{1}{3}C_1 = 9{\cdot}07 \times 10^{43}\ \text{g. cm.}^2; \qquad \tfrac{2}{3}A + \tfrac{1}{3}C = 80{\cdot}6 \times 10^{43}\ \text{g. cm.}^2;$$
$$A_1/A = 0{\cdot}112; \qquad \epsilon = 0{\cdot}00260.$$

Then

$$\frac{\varpi}{\varpi_0} = 0{\cdot}9940.$$

If $\varpi_0 = 9''{\cdot}2272$, $\varpi = 9''{\cdot}172$, which is far *less* than the observed value. Kelvin remarked that the reduction is independent of the thickness of the crust, which would make it independent of A_1. This is not so, but he appears to have been thinking of thin crusts, which were still popular when he wrote, and if we take 1/300 for ϵ, as he did, and A_1/A nearly 1 the reduction is by about 1 part in 23, which is what he found.

The correction depends on only two data for the core, A_1 and ϵ. The former is well determined by a very direct calculation. ϵ depends on the use of a hydrostatic theory, which is certainly not exact, and the results could be brought into agreement by taking ϵ three times as great as in the above calculation. But this would imply greater departures from hydrostatic stress in the shell than are indicated anywhere else, and just outside the core is the last place where we should expect them.

Lamb's analysis appears to assume uniform density for the core, but he uses only Helmholtz's equations in the core, and these remain true if the density depends only on the pressure; this is probably true with sufficient accuracy.

The couples L, M in the case of the nutation have not quite the same amplitude; if θ is the obliquity of the ecliptic they can be represented by two pairs of couples

$$L_1 + iM_1 = \tfrac{1}{2}\kappa(\cos\theta + \cos 2\theta)e^{i(-\omega+n)t},$$
$$L_2 + iM_2 = \tfrac{1}{2}\kappa(\cos\theta - \cos 2\theta)e^{i(-\omega-n)t}.$$

---

* *Phil. Trans.*, A, **186**, 469, 1895.

† *M.N., Geophys. Suppl.*, **3**, 395–401, 1936.

If n is negative the fluidity of the core reduces the response to the former and increases that to the latter, in nearly the same ratio. The nutations in latitude and longitude will both be diminished, but no longer in the same ratio; and the diminution will still be too great.

The assumption of a rigid shell is the most doubtful part of the hypotheses. In Kelvin's problem, indeed, the bending of a thin shell of ordinary rigidity would make the conditions approximate to those of a completely fluid body, in which the period of the free nutation would be infinite. In the Earth the pressures associated with the variations of velocity in the core would presumably bend the crust and again lengthen the period, so that the estimated reduction of amplitude may be too great.

I have not examined this possibility quantitatively, but I have examined two others sufficiently to see that they are not helpful. The allowance for elasticity, treating the whole Earth as elastic, is easily made by the method given in *The Earth* in discussing the variation of latitude, and is found to give a correction of order n/ω times the main term, which is small compared with either of the present discrepancies. The lunar deflection of the vertical might give a systematic error in the estimated position of the Pole. But the whole amount of this * is of order 0″·008, and its systematic effect on the observed nutation would be of the order of the fluctuation of its values according as the Moon's orbit is more or less oblique to the equator than the ecliptic is. Thus, at worst, the systematic error to be expected from lunar deflections of the vertical is of order 0″·001.

The main conclusion is that the theoretical nutation, obtained by taking the Earth as rigid, is probably too large; allowance for fluidity of the core while taking the shell as rigid reduces it to well below the observed value; but allowance for elasticity of the shell at the same time might result in agreement. Rediscussion of the theoretical period of the Eulerian nutation, using modern data on the elasticity of the Earth, is also desirable. In view of the need for knowledge of the viscosity of the core, it would also be useful if the observations of the nutation were re-examined with the object of finding out whether there is any measurable lag in phase.

160 *Huntingdon Road,*
Cambridge :
1948 *March* 1.

* E. Przybyllok, *A.N.*, **218**, 85–88, 1923.

ERRATA

M.N., **107**, No. 3, R. d'E. Atkinson's paper :

P. 298, line preceding equation (18), *for* $\sin \frac{1}{2}\theta$ *read* $\sin \frac{1}{2}\phi$, and in equation (18) *for* $\cos \frac{1}{2}\theta$ *read* $\cos \frac{1}{2}\phi$.

P. 302, seventh, fifth and fourth lines from foot of page, *for* 1·7° *read* 2°·7, *for* $\pm 5°$ *read* $\pm 8°$, *for* ten-degree *read* 16-degree.

THE FIGURES OF THE EARTH AND MOON *

H. Jeffreys, F.R.S.

(Received 1948 January 7)

Summary

The paper consists of a general adjustment of the data relevant to the radius and ellipticity of the Earth, the lunar parallax and the differences of the moments of inertia of the Moon. The anomalies of gravity recently found to persist over distances of 10° and 30° imply similar anomalies in the deflection of the vertical and provide a means of estimating the additional uncertainty that they introduce. When this is taken into account it is found that the data are satisfactorily consistent. Attempts are made to find additional checks on the existence of the anomalies of gravity represented by harmonics of degrees 2 and 3 other than the main ellipticity term, but they are indecisive, and the final solution is a compromise between solutions with and without them. The chief changes from current values are a reduction of the Earth's equatorial radius from 6371·388 km. to 6371·099±0·116 km. (s.e.) and of the value of g at Potsdam from 981·274 gals. to 981·2606±0·0010 gals.; owing to recent work by the Anglo-Iranian Oil Company the British stations are now strongly connected with the new determination of the absolute value of g at Teddington. The change in the equatorial radius is due to the use of free-air instead of isostatic reductions; reasons are given why the latter may have introduced a systematic error.

* The full text of this paper is published in *M.N., Geophys. Suppl.*, **5**, No. 7, 1948.